New dimensions of *CIITA*

Walter Reith & Jeremy M Boss

CIITA **encodes the 'master regulator' of the expression of major histocompatibility complex class II genes. A new layer of complexity has been identified in the control of *CIITA* expression, which involves the formation of a complex three-dimensional chromatin structure promoted by interactions among many distant regulatory elements.**

The molecular mechanisms regulating the expression of *CIITA* have been the subject of intense research by immunologists for more than a decade because it encodes a transcriptional coactivator that functions as the 'master regulator' of the expression of major histocompatibility complex class II genes[1–3]. The results reported in this issue by Ni *et al.*[4] bring to light a new and unanticipated complexity in the regulation of interferon-γ (IFN-γ)-induced *CIITA* expression by showing that it involves a series of five distant enhancers that promote the formation of a complex and dynamic three-dimensional chromatin structure.

It is now well established that transcription of *CIITA* is regulated by several promoters[2,3,5]. Four promoters, pI, pII, pIII and pIV, have been defined in human *CIITA* (**Fig. 1**). Each of these promoters is responsible for distinct tissue-specific expression modes of *CIITA*[2,3]. The promoters pI and pIII are responsible for myeloid- and lymphoid-specific expression patterns, respectively[6]. The specific function of pII is not yet known. The promoter pIV is the main IFN-γ-responsive promoter functioning in nonhematopoietic cells[7]. The finding that triggered the studies of Ni *et al.*[4] was that reporter gene constructs driven by the known regulatory sequences of pIV do not show dependency on BRG1, an ATP-dependent chromatin-remodeling factor shown before to be required for IFN-γ-induced expression of endogenous *CIITA*[8,9]. This prompted a search for distant BRG1-dependent enhancers required for IFN-γ-induced activation of pIV.

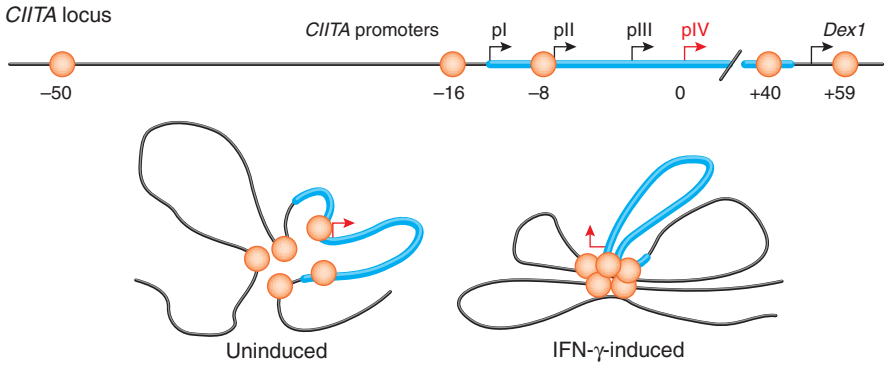

Figure 1 The *CIITA* locus and its four promoters, pI, pII, pIII and pIV. The thicker cyan line represents the entire *CIITA* gene from pI through to its last exon. Orange globes indicate the relative locations of the newly identified BRG1-dependent distal enhancers that collectively regulate IFN-γ-induced expression through pIV. In the uninduced state, weak or transient interactions between several of the enhancers and pIV occur. After IFN-γ induction, the interactions between the enhancers, and between the enhancers and pIV, are stabilized to form a discrete structure required for *CIITA* expression. The gene encoding dexamethasone-induced transcript (*Dex1*) is adjacent to the 3′ end of *CIITA*. Positions below *CIITA* are numbered in kilobases relative to pIV.

To pinpoint candidate enhancers, the authors first did chromatin-immunoprecipitation analysis and chromatin immunoprecipitation coupled to microarrays[4]. They used these approaches to identify regions in the *CIITA* locus that have IFN-γ-induced histone modifications associated with gene activation (acetylation of histones H3 and H4; methylation of lysine 4 of H3), that are associated with a histone acetyltransferase (p300) linked to IFN-γ-induced *CIITA* expression, and/or that are bound by transcription factors (STAT1 and IRF1) known to mediate IFNγ-induced *CIITA* expression[10]. They have identified five candidate enhancers spread over a 110-kilobase region encompassing the entire *CIITA* gene (**Fig. 1**). To show that these five regions indeed function as transcriptional enhancers required for IFN-γ-induced *CIITA* expression, they have done an impressive series of functional experiments with an elegant and sophisticated reporter gene system that relies on the engineering and transfection of bacterial artificial chromosome constructs containing 194 kilobases of genomic DNA from the *CIITA* locus. Finally, they use the chromatin conformation capture approach to demonstrate that the newly identified distal enhancers engage in many long-distance interactions with each other and with pIV to generate a complex and dynamic three-dimensional chromatin structure. The results suggest that in noninduced cells or in the absence of BRG1, the long-distance chromatin interactions are weak, transient or present in only a fraction of the cells (**Fig. 1**). However, the presence of BRG1 and/or exposure of the cells to IFN-γ promotes stabilization and remodeling of the three-dimensional structure (**Fig. 1**). Remodeling of the chromatin structure seems to be a requirement for CIITA expression.

Walter Reith is in the Department of Pathology and Immunology, University of Geneva Medical School, CH-1211 Geneva, Switzerland. Jeremy M. Boss is in the Department of Microbiology and Immunology, Emory University School of Medicine, Atlanta, Georgia 30322, USA.
e-mail: walter.reith@medecine.unige.ch

Until now, the individual promoters of the *CIITA* gene were believed to function as independent units and therefore have generally been presented as separate 'boxes' arrayed along a linear DNA molecule (**Fig. 1**, top line). However, the results reported by Ni *et al.*[4] now show that this one-dimensional and promoter-centric view of the regulatory region of *CIITA* needs to be revised. It is evident from their work that full understanding of the complexity of *CIITA* gene regulation must integrate the establishment and function of long-distance and dynamic chromatin interactions between regulatory elements that can be situated more than 100 kilobases apart. This view is becoming more common with genes that, like *CIITA*, were once thought to be regulated exclusively by their promoter-proximal regulatory regions[11,12]. Examples of these include the major histocompatibility complex class II genes that CIITA regulates, for which CIITA itself participates in long-range interactions with insulator-binding factors[13].

Future research will probably concentrate on the establishment and function of chromatin structures at the *CIITA* locus. In IFN-γ-induced *CIITA* expression, many important questions remain. At the top of the list are questions about the precise function of BRG1: does it move the nucleosomes to allow STAT1 and IRF1 binding or are other proteins involved? At present, the identity of the proteins that mediate the establishment of the long-distance chromatin loops between the distal enhancers and pIV remains unknown. Although such long-distance loops are indeed formed and required, it is not apparent why the proximal promoter regulatory elements at pIV are not sufficient for activation. One possibility suggested by the data is that repressive mechanisms are at work to ensure that the region cannot be activated without the aid of the other enhancer elements. Finally, it will be imperative to determine whether the lessons learned from IFN-γ-induced cells are also relevant to the regulation of *CIITA* in key 'professional' antigen-presenting cells, including dendritic cells, macrophages and B cells, and in cortical and medulary thymic epithelial cells. Are three-dimensional chromatin structures also critical in regulating *CIITA* expression in antigen-presenting cells and thymic epithelial cells? Are the structures formed in these cells similar to or different from those linked to IFN-γ-induced cells? Are the same or different distal enhancers involved in different cell types? The answers to these questions will provide fascinating new insights into the molecular mechanisms that regulate *CIITA* expression and thereby control antigen presentation mediated by major histocompatibility complex class II. Progress in these directions will contribute to propelling the regulation of *CIITA* expression to the forefront of the mammalian gene-regulatory systems that have been delineated genetically and biochemically in the greatest detail.

1. Steimle, V., Otten, L.A., Zufferey, M. & Mach, B. *Cell* **75**, 135–146 (1993).
2. Wright, K.L. & Ting, J.P. *Trends Immunol.* **27**, 405–412 (2006).
3. Leibundgut-Landmann, S. *et al. Eur. J. Immunol.* **34**, 1513–1525 (2004).
4. Ni, Z., Abou El Hassan, M., Xu, Z., Yu, T. & Bremner, R. *Nat. Immunol.* **9**, 785–793 (2008).
5. Muhlethaler-Mottet, A., Otten, L.A., Steimle, V. & Mach, B. *EMBO J.* **16**, 2851–2860 (1997).
6. LeibundGut-Landmann S., Waldburger, J.M., Reis e Sousa, C., Acha-Orbea, H. & Reith, W. *Nat. Immunol.* **5**, 899–908 (2004).
7. Waldburger, J.M., Suter, T., Fontana, A., Acha-Orbea, H. & Reith, W. *J. Exp. Med.* **19**, 393–406 (2001).
8. Mudhasani, R. & Fontes, J.D. *Mol. Cell. Biol.* **22**, 5019–5026 (2002).
9. Pattenden, S.G., Klose, R., Karaskov, E. & Bremner, R. *EMBO J.* **21**, 1978–1986 (2002).
10. Morris, A.C., Beresford, G.W., Mooney, M.R. & Boss, J.M. *Mol. Cell. Biol.* **22**, 4781–4791 (2002).
11. de Laat, W. & Grosveld, F. *Chromosome Res.* **11**, 447–459 (2003).
12. Schoenborn, J.R. *et al. Nat. Immunol.* **8**, 732–742 (2007).
13. Majumder, P., Gomez, J.A., Chadwick, B.P. & Boss, J.M. *J. Exp. Med.* **205**, 785–798 (2008).

Erg in stem cells: a function emerges

Ellen V Rothenberg

Transcription factors of the Ets family are important for mammalian development. A genetic screen now finds that the Ets family member Erg is essential for definitive hematopoiesis and adult hematopoietic stem cell function.

The transcription factor Erg has presented a challenging problem for researchers for over two decades since its discovery[1]. Strongly linked to the pathogenesis of many cancers and noteworthy in its expression pattern, *in vitro* transcriptional activity and genomic linkages, the *Erg* proto-oncogene has nevertheless resisted conventional reverse-genetic approaches for defining its normal functions *in vivo*. In this issue of *Nature Immunology*, Loughran *et al.* now report a considerable advance toward the clarification of this gene's importance[2]. Using the classic forward-genetics approach of a phenotypic screen on a 'sensitized background' (discussed below), these investigators have obtained a missense mutation of *Erg* that is probably the first lesion to cause a distinct loss of function of this transcription factor. This mutation turns out to have profound effects on definitive hematopoiesis and especially on the hematopoietic stem cell compartment. *Erg* gene dosage is shown to be so critical that a strong effect on stem cell function is present even in the heterozygous state.

Erg has long been suspected of being involved in self-renewal–associated proliferation because of its many contributions to cancer. Translocations that link the Erg DNA-binding domain to other genes or place Erg expression under inappropriate control are probably causal factors in Ewing's sarcoma and prostate cancer[3], and aberrantly high Erg expression has been linked to hematopoietic cancers, including myeloid and T lymphoblastic leukemias. *ERG* maps to the Down's syndrome critical region of chromosome 21 (chromosome 16 in the mouse), where an increase from diploid to triploid gene dosage has also been suggested as a possible contributor to Down's syndrome–associated megakaryocytic leukemia[4]. However, oncogenesis is obviously not the normal function of Erg *in vivo*. During embryonic development, Erg expression is associated with mesoderm and particularly with developing endothelium and cartilage, where it seems to have a specific function in the regulation of endothelial genes[5,6] and chondrocyte genes[7]. In hematopoiesis, Erg has been linked mainly to megakaryocytic gene expression[4], although its expression pattern, including that in stem cells, T cell precursors and B cell precursors, has hinted at a broader function. However, the mutations available to assess such a function have so far been mainly oncogenic translocations, for which the gain of abnormal function complicates the effects of any loss of normal function.

Structurally, Erg is very similar to another

Ellen V. Rothenberg is in the Division of Biology, California Institute of Technology, Pasadena, California 91125, USA.
e-mail: evroth@its.caltech.edu

nature immunology

The chromatin-remodeling enzyme BRG1 coordinates *CIITA* induction through many interdependent distal enhancers

Zuyao Ni[1,2], Mohamed Abou El Hassan[1,2], Zhaodong Xu[1], Tao Yu[1] & Rod Bremner[1]

The chromatin-remodeling enzyme BRG1 is critical for interferon-γ (IFN-γ)-mediated gene induction. Promoter-proximal elements are sufficient to mediate BRG1 dependency at some IFN-γ targets. In contrast, we show here that at *CIITA*, which encodes the 'master regulator' of induction of major histocompatibility complex class II, distal elements conferred BRG1 dependency. At the uninduced locus, many sites formed BRG1-independent loops. One loop juxtaposed a far downstream element adjacent to a far upstream site. Notably, BRG1 was recruited to the latter site, which triggered the appearance of a histone 'mark' linked to activation. This subtle change was crucial, as subsequent IFN-γ-induced recruitment of the transcription factors STAT1, IRF1 and p300, as well as histone modifications, accessibility and additional loops, showed BRG1 dependency. Like BRG1, each remote element was critical for the induction of *CIITA* expression. Thus, BRG1 regulates *CIITA* through many interdependent remote enhancers, not through the promoter alone.

CIITA (also called MHC2TA; A000657), the 'master regulator' of gene expression of major histocompatibility complex (MHC) class II, is a coactivator that induces MHC class II promoters[1]. Constitutive *CIITA* expression in antigen-presenting cells such as B lymphocytes and dendritic cells ensures constant MHC class II expression, and in non–antigen-presenting cells, MHC class II loci are silent but are readily induced through induction of *CIITA* transcription mediated by interferon-γ (IFN-γ; A001238)[1]. Defects in *CIITA* regulation cause bare lymphocyte syndrome, a severe immune deficiency, and are linked to other human diseases, including cancer, multiple sclerosis, arthritis and myocardial infarction[1–3]. As well as its broad clinical relevance, *CIITA* is an excellent model for studying the regulation of IFN-γ-stimulated genes (ISGs) and rapid gene induction in general.

IFN-γ inhibits proliferation, virus infection and tumorigenesis[4,5]. It is secreted by activated T cells, natural killer cells and some dendritic cells but acts on most cell types[5,6]. IFN-γ triggers the activation and nuclear translocation of the transcription factor STAT1, which induces many ISGs[5]. One STAT1 target is the gene encoding the transcription factor IRF1; both STAT1 and IRF1 then act together to induce *CIITA*[7–9]. *CIITA* has four alternative first exons (I–IV), but the main IFN-γ-responsive promoter is pIV (ref. 10). The promoters pI and pIII are active mainly in dendritic cells and B cells, respectively. Unlike other mRNA molecules, type II transcripts are not found in the mouse and are of extremely low or negligible abundance in human tissues and cell lines[10], except in some melanomas[11]. As with most genes, studies of IFN-γ-mediated *CIITA* induction have focused on proximal elements and, except for a region around pII (refs. 11,12), little consideration has been given to distal elements.

BRG1 is the ATPase 'engine' that drives the chromatin-remodeling complex SWI-SNF (also called BAF). It is conserved in species from yeast to humans and regulates many genes and biological processes[13]. SWI-SNF does not have sequence-specific binding activity but is recruited to gene targets by DNA-binding proteins[14]. Defects in BRG1 and other SWI-SNF components are linked to cancer[15], so understanding its mechanism of action is of broad interest. Most work on BRG1 has focused on promoter-proximal effects. Gene induction by nuclear receptors[16], viral induction of the *Ifnb* promoter[17] and differentiation-associated induction of adipocyte promoters[18] are a few of the many examples of this. In several cases, replicating reporters, which correctly assemble octameric nucleosomes in S phase, or promoter templates, properly associated with chromatin *in vitro*, show BRG1-dependent regulation[14,19–22]. Such data do not exclude the possibility of involvement of BRG1 at distal sites, but few studies have addressed this issue. During T cell development, BRG1 regulates a silencer at the *Cd4* locus, but this element is only 2 kilobases (kb) from the promoter and the events it controls are unknown[23]. BRG1 binds a cluster of genes encoding interleukin 5 (IL-5), IL-4 and IL-3 (ref. 24), but whether it is essential for regulation, and its precise function if it is, is unknown. The gene encoding mouse β-globin is a differentiation locus where BRG1 acts remotely. Here, BRG1 binds hypersensitive sites in the locus-control region of this gene[25,26] and facilitates acetylation of histone H3 and DNase I accessibility, prevents methylation of CpG

[1]Genetics and Development Division, Toronto Western Research Institute, University Health Network. Department of Ophthalmology and Vision Sciences, Department of Laboratory Medicine and Pathobiology, University of Toronto, Toronto, Ontario M5T 2S8, Canada. [2]These authors contributed equally to this work. Correspondence should be addressed to R.B. (rbremner@uhnres.utoronto.ca).

Received 13 December 2007; accepted 21 April 2008; published online 25 May 2008; doi:10.1038/ni.1619

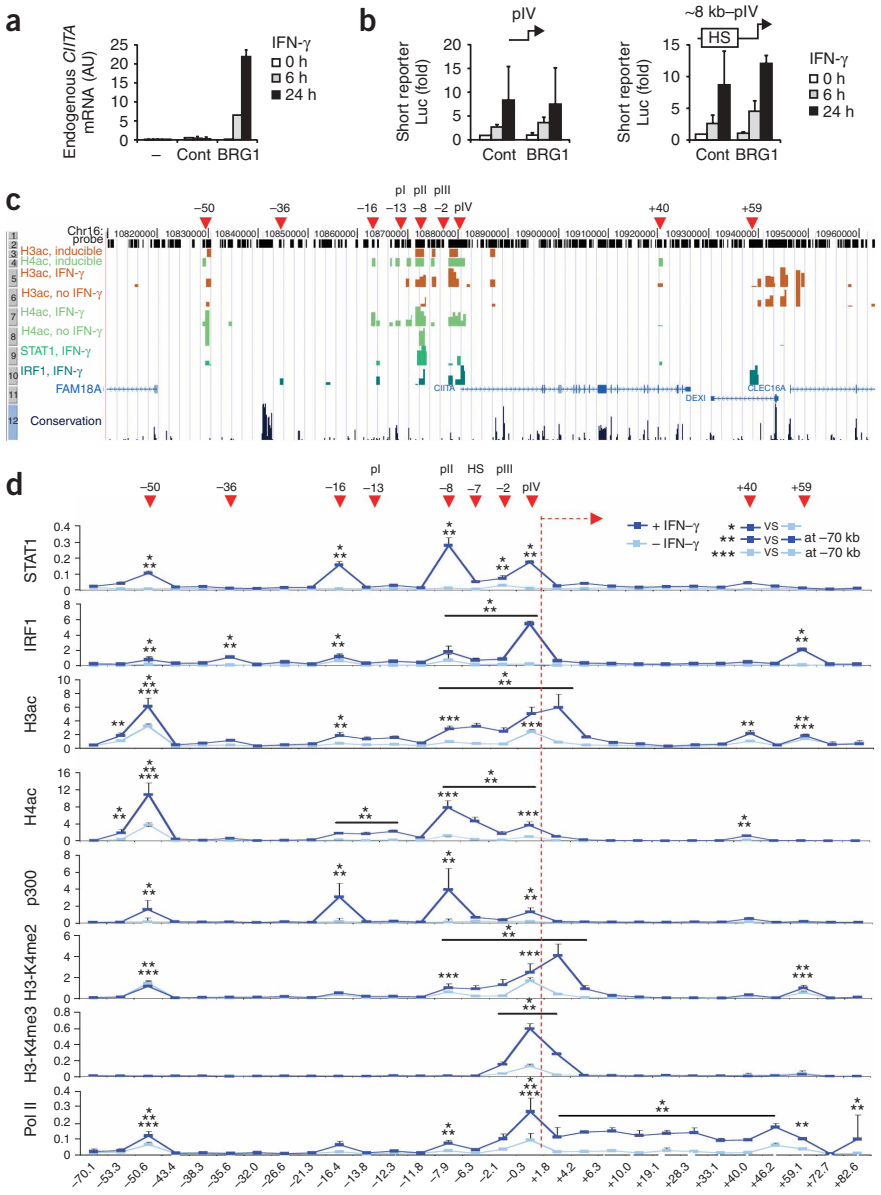

Figure 1 Distal IFN-γ-induced chromatin activity at *CIITA*. (**a**) Real-time PCR analysis of *CIITA* expression in SW13 cells transduced with adenoviral vectors and exposed to IFN-γ for 0–24 h (key). –, no virus; Cont, Ad-GFP control virus; BRG1, Ad-BRG1 virus; AU, arbitrary units (relative to β-actin). (**b**) Activity of firefly luciferase reporters (bent arrows at top), containing pIV alone (left) or pIV plus about 8 kb of 5′ sequence (right; ~8 kb-pIV), in SW13 cells in the presence of control plasmid (Cont; pBJ5) or BRG1-expressing plasmid (BRG1), after treatment with IFN-γ for 0–24 h (key); firefly luciferase activity (Luc) is normalized to that of renilla luciferase. HS, DNase I–hypersensitive site about 7 kb upstream of pIV. (**c**) Analysis across *CIITA* by ChIP on tiled genome array. Row 1, position (in base pairs) across 153 kb of chromosome 16 (Chr16); numbers above indicate distance of sites in kb upstream (–) or downstream (+) of pIV. Row 2, probe (black bars) and excluded repetitive positions. Rows 3 and 4, positions of significant H3ac or H4ac induction ($P < 0.0001$). Rows 5–10, $\log_2$ 'fold' value significantly above input signal ($P < 0.0001$) with anti-H3ac (rows 5,6), anti-H4ac (rows 7,8), anti-STAT1 (row 9) and anti-IRF1 (row 10), with IFN-γ (rows 5,7,9,10) or without IFN-γ (rows 6,8); binding of STAT1 and IRF1 without IFN-γ was negative (data not shown). Row 11, gene positions. Row 12, conservation across 17 vertebrates. (**d**) ChIP–quantitative PCR data (presented as % input) for various factors or histone modifications (vertical axes) at sites across *CIITA* (horizontal axis). Pol II, RNA polymerase II. *, ** and ***, values over fivefold above background at the control site at –70 kb; $P < 0.01$ for comparisons at top right (vs, versus). Red downward arrowheads (**c**,**d**) indicate sites of chromatin activity (distance from pIV in kb); above, positions of pI, pII, pIII and a hypersensitive site identified in a glioblastoma cell line[12]. Data (mean and s.d.) are representative of at least three experiments.

dinucleotides and promotes gene expression[27], although recruitment of the transcription factors GATA1 and NF-E2 is BRG1 independent[28]. Whether BRG1 has remote effects at other loci, particularly at rapidly induced genes, is unknown. Enhancers often function by looping and, notably, yeast SWI-SNF stimulates looping on nucleosomal arrays assembled *in vitro*[29]. However, whether SWI-SNF is sufficient or necessary to stimulate looping *in vivo* is unclear.

BRG1 has been linked to IFN-γ-mediated induction of *CIITA*[30], which raises the possibility of another mechanism by which BRG1 might block tumorigenesis by immune surveillance. BRG1 regulates many gene targets induced by IFN-γ, IFN-α and IL-6 (refs. 9,22,31–34). These pathways activate STAT complexes, and in each case, BRG1 is essential for the STAT proteins to access promoters[9,32,34]. Moreover, studies of the ISGs *IFITM3* and *IFITM1* have shown that promoter-proximal reporters are SWI-SNF dependent, exactly like the endogenous genes[22,32]. These data all support a 'promoter-centric' view of BRG1 action at ISGs. Here we show that the *CIITA* promoter was insufficient to confer BRG1 dependency. Instead, BRG1 coordinated engagement of a multienhancer complex spread over more than 100 kb. Our data considerably alter the understanding of *CIITA* regulation, define principals that may be broadly relevant at ISGs, identify previously unknown elements that could have variants linked to human disease, tie BRG1 to remote effects, including looping at rapidly induced genes, and provide an ideal model for studying the distal effects of SWI-SNF.

RESULTS

Evidence for distal effects at *CIITA*

Proper nucleosome deposition requires DNA replication and, notably, published studies have indicated a replication requirement for SWI-SNF-dependent induction of two ISGs[22,32]. However, we found that even with a replicating vector, IFN-γ induction of *CIITA* pIV was BRG1 independent, unlike that of the endogenous locus (**Fig. 1a**,**b**). The addition of 8 kb of 5′ sequence, including a DNase I–hypersensitive site at about –7 kb (distances are presented here relative to the start site at pIV)[12], did not confer BRG1 dependency (**Fig. 1b**). Thus, we hypothesized that the BRG1 dependency at *CIITA* may result from remote effects.

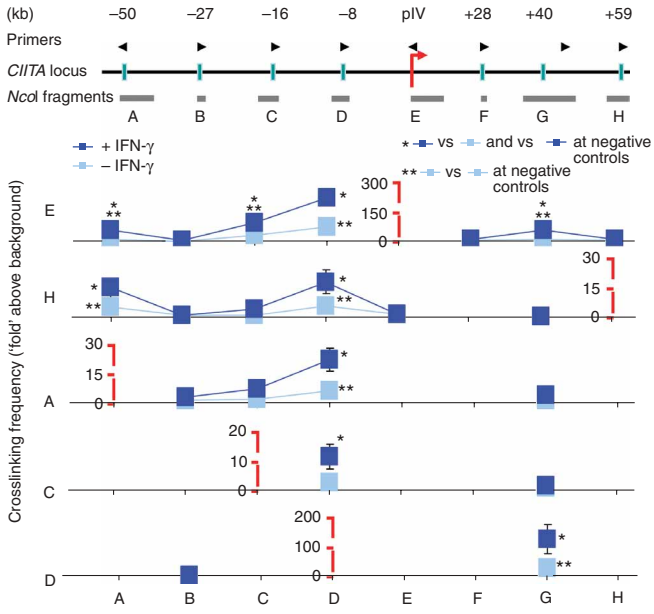

Figure 2 Basal and IFN-γ-induced looping at *CIITA*. Quantitative chromatin conformation capture assay of chromatin from HeLa cells left untreated or exposed to IFN-γ for 6 h. Top, position of primers and *Nco*I fragments. Data represent the interaction of one reference *Nco*I fragment with other *Nco*I fragments, assessing all 15 possible interactions between –50 kb, –16 kb, –8 kb, pIV, +40 kb and +59 kb (fragments A, C, D, E, G and H), as well as many elements also tested for interaction with the irrelevant regions at –27 kb or +28 kb (fragments B and F). Left (E, H, A, C, D), reference fragment; small red vertical lines indicate its position and the scale of the interaction. A simplified heat-map matrix and a diagram summarizing the data are in **Supplementary Figure 2**. * and **, $P < 0.05$, relative to background interactions (comparisons, top right). Data (mean ± s.d.) are representative of at least three experiments.

To locate remote IFN-γ-responsive enhancers, we mapped STAT1 and IRF1 sites at *CIITA* and other ISGs by chromatin immunoprecipitation (ChIP) on tiled genome arrays. We also mapped acetylated histone H3 (H3ac) and H4ac marks, which are common at active or 'poised' regulatory elements[35,36]. Future studies should provide genome-scale data; here we focused on *CIITA*. For the ChIP on tiled genome arrays, we used chromatin from HeLa cells left untreated or exposed to IFN-γ for 6 h, which represents the peak of transcription factor binding and acetylation at *CIITA* pIV (ref. 16). We found many IFN-γ-responsive sites across a 109-kb window, as indicated by binding of STAT1 and IRF1 and induced H3ac and/or H4ac peaks (**Fig. 1c**). We detected constitutive H3ac signals at *DEX1*, a constitutively transcribed non-ISG 3′ of *CIITA* on the opposite strand (**Fig. 1c**). ChIP–quantitative PCR at 29 locations across 153 kb verified activator binding and/or H3-H4 acetylation at sites –50, –16, –8, +40 and +59 kb relative to pIV, whereas other sites showed low or no signals (**Fig. 1d** and **Supplementary Table 1** online). We confirmed small amounts of IRF1 bound at –36 kb but not at –26 kb. The site at –8 kb overlaps the weak or inactive human-specific pII promoter and is close to a previously mapped hypersensitive site[12]; indeed, these may be coincident, as the latter has not been 'fine mapped'. We detected transcripts initiating only at pIV in the cells used here (data not shown). The lack of pII activity in mice and its nearly undetectable activity in humans[10], published reporter assays showing it acts as a context-specific enhancer or silencer[11,12], and our analyses here (**Fig. 1** and discussed below) suggest this region may be mainly a remote regulatory element rather than a promoter.

The transcription factor p300 has been linked to histone acetylation at pIV (ref. 16). ChIP–quantitative PCR showed that p300 was also inducibly recruited to remote sites (–50 kb, –16 kb and –8 kb; **Fig. 1d**). Dimethylated lysine 4 of histone H3 (H3-K4me2) marks accessible active regions[37] and was constitutively present in untreated or IFN-γ-treated cells at sites at –50 kb, –8 kb and +59 kb (**Fig. 1d**). H3-K4me2 binding was induced at pIV after IFN-γ treatment. H3-K4me3 marks promoters[37] and, indeed, we detected it only at pIV, and the abundance of bound H3-K4me3 was also increased by IFN-γ treatment (**Fig. 1d**). A low basal amount of RNA polymerase II was bound at –50 kb and pIV, and after induction, we detected it across the entire *CIITA* gene (**Fig. 1d**). RNA polymerase II was also induced at the sites at –50 kb and –8 kb (**Fig. 1d**), but its absence at intervening sites, the presence of H3-K4me3 at pIV only and the lack of RNA transcripts at the upstream regions, even with sensitive PCR detection (Z.N. and R.B., unpublished data), challenged the idea of transcription initiation upstream of pIV and suggested that distal elements may loop and contact pIV. Indeed, by chromatin conformation capture assay[38] and qualitative gel-based analysis of amplified ligation products, we detected robust IFN-γ-induced contact between pIV and the elements at –50 kb or –8 kb, and between –16 kb and –50 kb (**Supplementary Fig. 1** online). No interactions were detected in the absence of ligase or between pIV and irrelevant sequences. This qualitative approach 'ignores' differences in PCR efficiency and misses weaker interactions detectable with additional cycles, so we used quantitative chromatin conformation capture assays to confirm the data, extend it to assess all possible interactions and measure the strength of various contacts (**Fig. 2** and **Supplementary Fig. 2** online). We assessed a total of twenty-one interactions between eight fragments, including all fifteen between the six regulatory elements and six more with two negative control sites at –27 kb and +28 kb that showed no binding of STAT1 or IRF1 or histone acetylation. Of all twenty-one interactions tested, we noted eight constitutive contacts: four weak (between the sites at –50 kb and –8 kb (–50:–8), –50:+59, –8:+59, pIV:+40), three moderate (–50:pIV, –16:pIV, –8:+40) and one strong (–8:pIV). IFN-γ enhanced all those pre-existing basal interactions and stimulated one new contact (–16:–8). The absence of thirteen of twenty-one possible interactions in the basal state and twelve of twenty-one in the induced state, including the complete absence of looping to irrelevant sites at –27 or +28 kb, indicated specificity. There was also no correlation between the distance separating each fragment and looping either in untreated HeLa cells ($R^2 = 0.09$) or IFN-γ-treated HeLa cells ($R^2 = 0.08$; **Supplementary Fig. 3, Table 2** and **Methods** online). Thus, distal elements identified by ChIP on tiled genome arrays showed specific constitutive and enhanced or additional IFN-γ-induced contacts with pIV and/or each other.

BRG1-independent and BRG1-dependent chromatin alterations

Next, we sought to determine if BRG1 bound to any of the newly identified distal sites. BRG1 was constitutively bound to the sites at –50, –16, –8 and +59 kb (**Fig. 3a**) and with pIV, as shown before[30]. There was negligible recruitment of BRG1 at intervening sites. These data support the idea that BRG1 acts at remote *CIITA* sites and offer an explanation for the failure of short reporters to show BRG1-dependent IFN-γ induction (**Fig. 1b**).

BRG1 is required for all IFN-γ-induced factor binding and histone modifications at *CIITA* pIV and at other cytokine-induced promoters[9,34]. Thus, we sought to determine whether IFN-γ-induced events at remote sites were also BRG1 dependent. The assays reported above

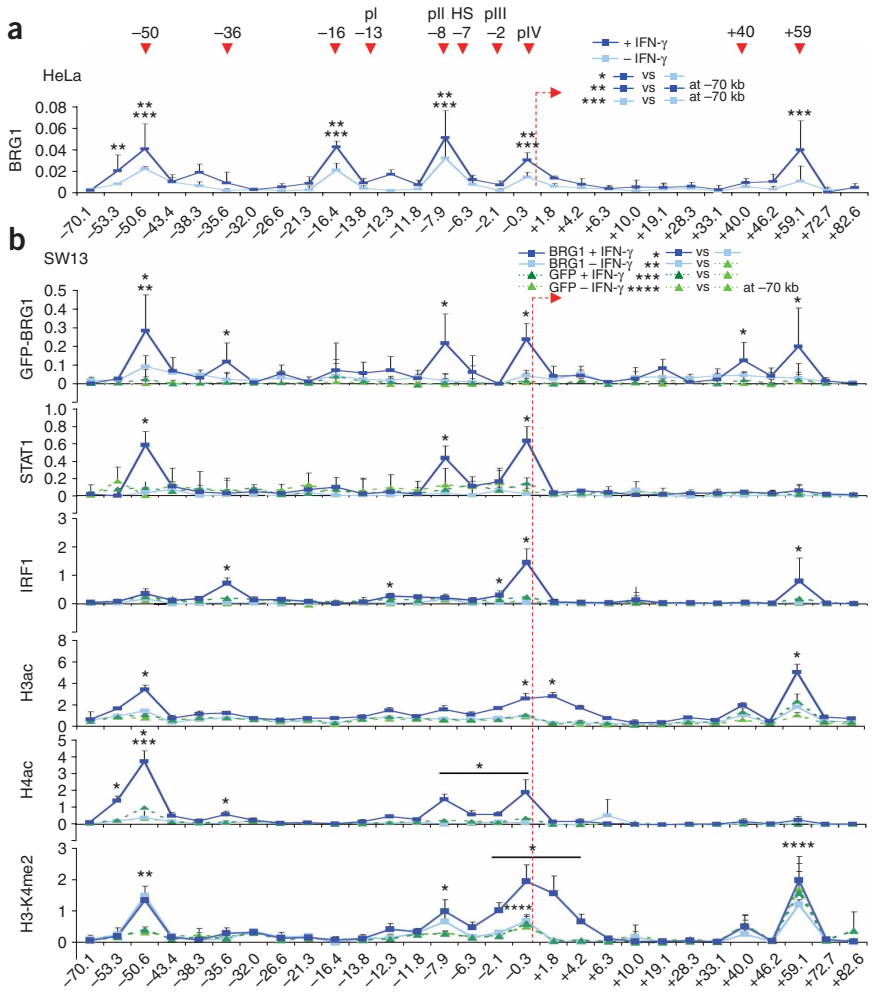

Figure 3 BRG1-dependent distal events at *CIITA*. (**a**) ChIP–quantitative PCR of chromatin from untreated or IFN-γ treated HeLa cells, analyzed with anti-BRG1. (**b**) ChIP–quantitative PCR analysis (presented as % input) of chromatin from SW13 cells transduced with Ad-GFP-BRG1 or Ad-GFP, and left untreated or stimulated with IFN-γ for 6 h. *, **, *** and ****, values fivefold above background signal at the control site at –70 kb ($P < 0.01$ for comparisons at top right). Red dashed arrows indicate the transcription start at pIV; red downward arrowheads at top indicate the position (in kb) of remote elements from pIV; above, positions of pI, pII, pIII and a hypersensitive site identified in a glioblastoma cell line[12]. Data (mean and s.d) are representative of at least three experiments.

used BRG1-expressing HeLa cells, so we used BRG1-deficient human adrenal carcinoma SW13 cells transduced with adenoviral vectors expressing green fluorescent protein (GFP; Ad-GFP) or GFP-tagged BRG1 (Ad-GFP-BRG1)[9]. The abundance of virally expressed BRG1 matched endogenous HeLa amounts[9]. We made four important observations. First, we detected a constitutive BRG1-independent, IFN-γ-independent H3-K4me2 mark at +59 kb (**Fig. 3b**). It was unaffected by IFN-γ, consistent with only marginal induction in HeLa cells (**Figs. 1d** and **3b**). Second, when added, BRG1 was recruited constitutively to the site at –50 kb (**Fig. 3b**). This result differed slightly from that of HeLa cells, in which BRG1 was also present constitutively at other remote sites (**Fig. 3a**), perhaps because of stronger basal looping (discussed below; **Supplementary Fig. 2**). Third, BRG1 binding at –50 kb triggered a second H3-K4me2 mark also at –50 kb, which remained unchanged after treatment with IFN-γ, as was the case in HeLa cells (**Figs. 1d** and **3b**). This effect is consistent with published data linking BRG1 to histone lysine methylation[39,40]. This unique BRG1-induced event may prime *CIITA* for IFN-γ responsiveness. Finally, in BRG1-deficient cells, IFN-γ did not alter factor binding or histone modifications at any remote element, but in BRG1-reconstituted cells, IFN-γ induced extensive binding of BRG1, STAT1 and IRF1, as well histone acetylation and methylation similar to that in HeLa cells (**Figs. 1d**, **3** and **Supplementary Table 1**). An exception was the site at –16 kb, which showed changes in HeLa cells but not in SW13 cells.

Next, we sought to determine if BRG1 altered *in vivo* accessibility to DNase I at remote elements. In BRG1-deficient cells, DNase I digestion was identical with or without IFN-γ at all loci tested (**Fig. 4**). In contrast, although the addition of BRG1 did not affect basal accessibility to DNase I, it increased IFN-γ-induced accessibility at –50 kb, –8 kb and pIV (**Fig. 4**). Consistent with the absence of other IFN-γ effects at –16 kb in SW13 cells, we found no DNAse I accessibility at this location. Accessibility at an irrelevant site at –70 kb was also unaffected (**Fig. 4**). Thus, perfect correlation exists between BRG1 binding and IFNγ-induced accessibility at the sites at –50 and –8 kb as well as pIV.

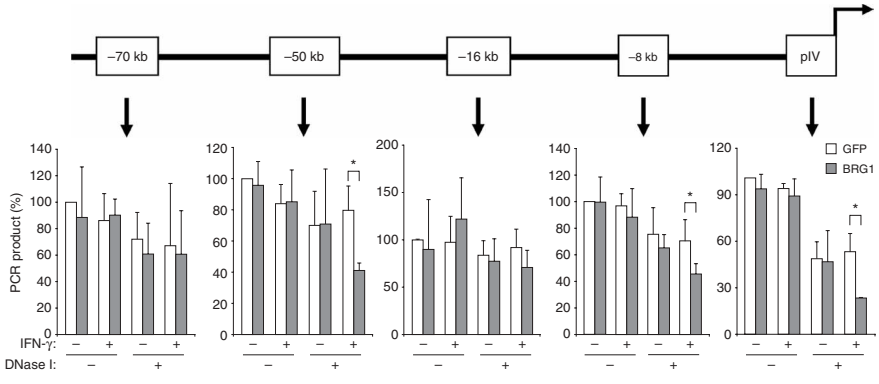

Figure 4 IFN-γ-induced accessibility at distal sites is BRG1 dependent. Quantitative PCR at various sites (above graphs) around the *CIITA* locus in SW13 cells transduced with Ad-GFP or Ad-GFP-BRG1 and left untreated or stimulated with IFN-γ for 6 h; nuclei were incubated with buffer (–) or DNase I (+). '100%' represents PCR product obtained from samples not exposed to IFN-γ or DNase I. *, $P < 0.05$. Data (mean and s.d.) are representative of three experiments.

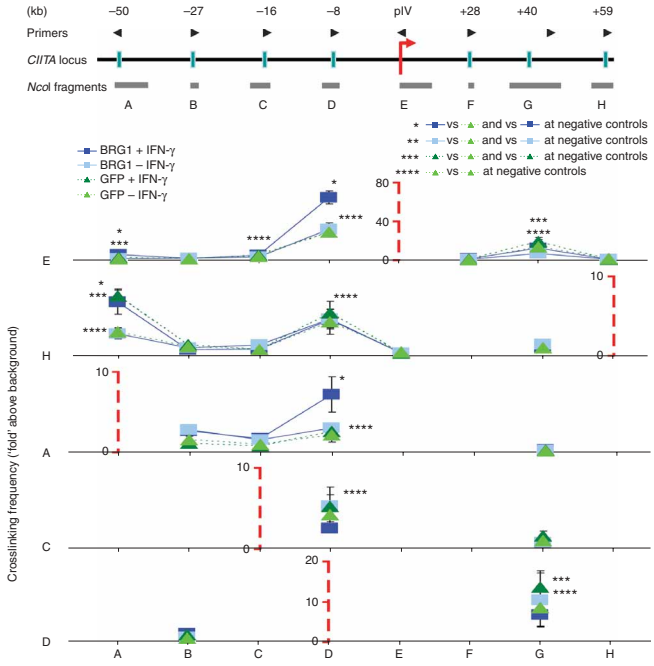

Figure 5 BRG1-dependent and BRG1-independent chromatin looping. Quantitative chromatin conformation capture assay of chromatin from SW13 cells transduced with Ad-GFP or Ad-GFP-BRG1 and left untreated or exposed to IFN-γ for 6 h (labels as described in **Fig. 2**). A simplified heat-map matrix and a diagram summarizing the data are in **Supplementary Figure 2**. *, **, *** and ****, $P < 0.05$, relative to background interactions (comparisons, top right). Data (mean and s.d.) are representative of three experiments.

BRG1 is required for IFN-γ-induced but not basal looping

Next, we used quantitative chromatin conformation capture assays to measure looping in the presence or absence of BRG1 and with or without IFN-γ (**Fig. 5** and **Supplementary Fig. 2**). In untreated BRG1-deficient cells, we detected eight of all twenty-one contacts tested (–50:+59, –50:–8, –16:–8, –16:pIV, –8:pIV, –8:+40, –8:+59 and pIV:+40). Notably, BRG1 did not affect this 'superstructure'; thus, its main effect was to induce H3-K4me2 at –50 kb (**Fig. 3b**). IFN-γ enhanced the constitutive –50:–8 and –8:pIV contacts in a BRG1-dependent way and stimulated a new –50:pIV contact more effectively in the presence of BRG1. IFN-γ enhancement of the –50:+59 contact was BRG1 independent. We confirmed several results by qualitative analysis (**Supplementary Fig. 4** online). As in HeLa cells, no contacts were made with the irrelevant sites at –27 kb or +28 kb, and the presence or absence of contacts did not correlate with distance between fragments (**Supplementary Fig. 3c**, **Table 2** and **Methods**). Constitutive and IFN-γ-induced DNA interactions were very similar in HeLa and SW13 cells (**Supplementary Fig. 2**). Basal *CIITA* transcript abundance was higher in HeLa cells than in SW13 cells, consistent with the unique presence of the constitutive –50:pIV contact, the stronger (that is, more frequent) contacts between elements and more histone modifications (**Supplementary Fig. 2**). Higher induced *CIITA* expression in HeLa cells correlated with stronger contacts and histone modifications at –16 kb that were absent in SW13 cells (**Supplementary Fig. 2**).

Remote elements confer BRG1 dependency on *CIITA* pIV

To test if the newly identified elements regulated promoter activity, we first inserted sequences of about 1 kb corresponding to the *cis* elements at –50 kb, –16 kb and –8 kb into a pIV-containing replicating luciferase reporter, alone or together. The element at –8 kb increased IFN-γ-induced pIV activity, whereas the elements at –16 kb and –50 kb repressed basal pIV activity, which was relieved by IFN-γ (**Supplementary Fig. 5** online). When all three were placed together, the repressive effect of the elements at –16 kb or –50 kb on basal activity was relieved and IFN-γ-responsiveness was equivalent to that seen with the element at –8 kb alone. These elements were not in their endogenous configuration, so these assays probably do not reflect their exact function *in vivo* but indicate that they can influence promoter activity.

To test function in a more relevant context, we used the bacterial artificial chromosome (BAC) CTD-2577P18 containing 194 kb of DNA flanking the entire *CIITA* locus. To quantify induction, we introduced an internal ribosome entry site–luciferase cassette into the 3′ untranslated region of *CIITA* (**Supplementary Fig. 6a** online). To facilitate the formation of chromatin of integrated or episomal BAC vectors, we incorporated a DNA replication origin[41]. We transfected SW13 cells with the modified vector (BAC-*CIITA*; **Supplementary Fig. 6b**) and selected stable clones in the aminoglycoside G418. We transduced two pools with Ad-GFP or Ad-GFP-BRG1, then left them untreated or exposed them to IFN-γ for 6, 24 or 48 h and normalized luciferase activity to protein content. We found IFN-γ-induced luciferase activity specifically in BRG1-expressing but not BRG1-deficient pools (**Fig. 6a**). We selected seventeen individual clones, of which eight contained BAC DNA, as assessed with primers for three BAC-specific regions (data not shown). For BAC-containing clones, we normalized luciferase activity to total protein content and then to the BAC copy number determined by quantitative PCR. BRG1 alone did not affect basal expression, as seen at the endogenous locus[9] (**Fig. 1a**). Most notably, whereas BRG1-deficient cells showed no or minimal induction, BRG1 conferred IFN-γ inducibility ($P < 0.05$; **Fig. 6b**). As expected, different clones showed variable induction, perhaps because of differences in the ratio of integrated to episomal

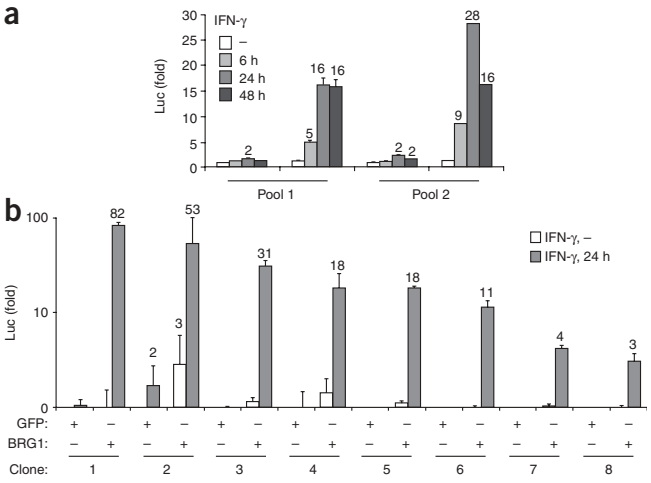

Figure 6 Remote regions confer BRG1 dependency on *CIITA*. Luciferase activity of SW13 cells transfected with the BAC-*CIITA* luciferase vector, selected in G418, then transduced with Ad-GFP or Ad-GFP-BRG1 as pools (**a**) or individual clones (**b**) and left untreated or exposed to IFN-γ (time, key). Numbers above bars indicate 'fold change' relative to the untreated Ad-GFP sample (no number indicates no change ('onefold')). Data (mean and s.d.) are representative of three experiments.

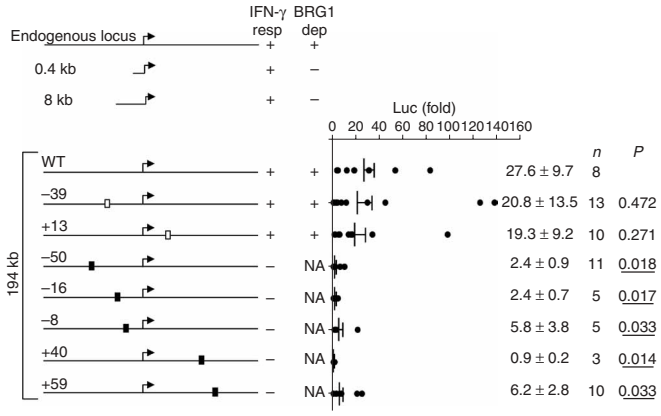

Figure 7 BRG1 and distal elements are required for *CIITA* induction. Left, IFN-γ responsiveness (resp) and BRG1 dependency (dep) of the endogenous *CIITA* locus and various reporter vectors. NA, not applicable; WT, wild-type. Data for endogenous locus and short reporters are from **Figure 1**. Right, data for large reporters: luciferase assay (as in **Fig. 6**) of lysates of SW13 colonies stably transfected with BACs lacking various sites (open boxes, controls; filled boxes, regulatory elements), presented as the 'fold change' in luciferase activity in IFN-γ-treated and BRG1-expressing cells relative to that of untreated Ad-GFP-expressing control cells. Long and short vertical lines indicate average and s.e.m., respectively (values presented at right); *n* represents the number of clones analyzed for each BAC; underlined *P* values indicate vectors with significantly impaired IFN-γ responsiveness relative to the wild-type vector, even in the presence of BRG1. Data represent the average of three replicate assays.

copies, the location of integrated copies, recombination with the endogenous locus and/or the frequency of disruption to BAC structure. But critically, the BRG1-dependent response of the BAC with either pools or many independent clones contrasted with that of small vectors induced independently of BRG1 (**Fig. 1b**) but matched the response of the endogenous locus, which was also BRG1 dependent (**Fig. 1a**). Thus, remote elements present in the 194-kb BAC conferred BRG1 dependency on *CIITA*.

Remote elements are required for *CIITA* induction

Next, we investigated the function of each remote enhancer. Using homologous recombination[42], we replaced about 1 kb of sequence at seven remote sites with a galactokinase (*galK*) selection marker (**Supplementary Fig. 6**), including the sites at –50 kb, –8 kb, +40 kb or +59 kb that showed chromatin activity in both HeLa and SW13 cells, the site at –16 kb that was active in HeLa cells, and the sites at –39 kb and +13 kb that were inactive in either context (**Figs. 1d** and **3** and **Supplementary Table 1**). We transfected SW13 cells with the modified BACs and selected G418-resistant clones. In addition to the 17 wild-type clones discussed above, 97 mutated BAC stable clones were generated. Of those 114 clones, 63 (55.3%) contained BAC DNA, as detected with primers for three BAC regions. We transduced clones with Ad-GFP-BRG1 or Ad-GFP, then left them untreated or exposed them to IFN-γ for 24 h and assessed luciferase activity. We normalized values to total protein content and BAC number as described above and plotted induction relative to that of untreated GFP-transduced cells (**Fig. 7**). As with the wild-type BAC, BRG1 alone did not affect basal expression and IFN-γ had no effect in GFP-transduced cells (data not shown). In BACs lacking control regions at –39 kb (the most conserved noncoding region at *CIITA*) or +13 kb, the range of BRG1-dependent IFN-γ responsiveness across many clones matched that of the wild-type BAC vector (**Fig. 7**), which indicated that BAC function was not compromised by *galK*. In contrast, removal of the sites at –50, –16, –8, +40 or +59 kb significantly impaired IFN-γ induction, even in the presence of BRG1 ($P < 0.05$; **Fig. 7**). The functional relevance of the site at –16 kb in SW13 cells is consistent with looping data

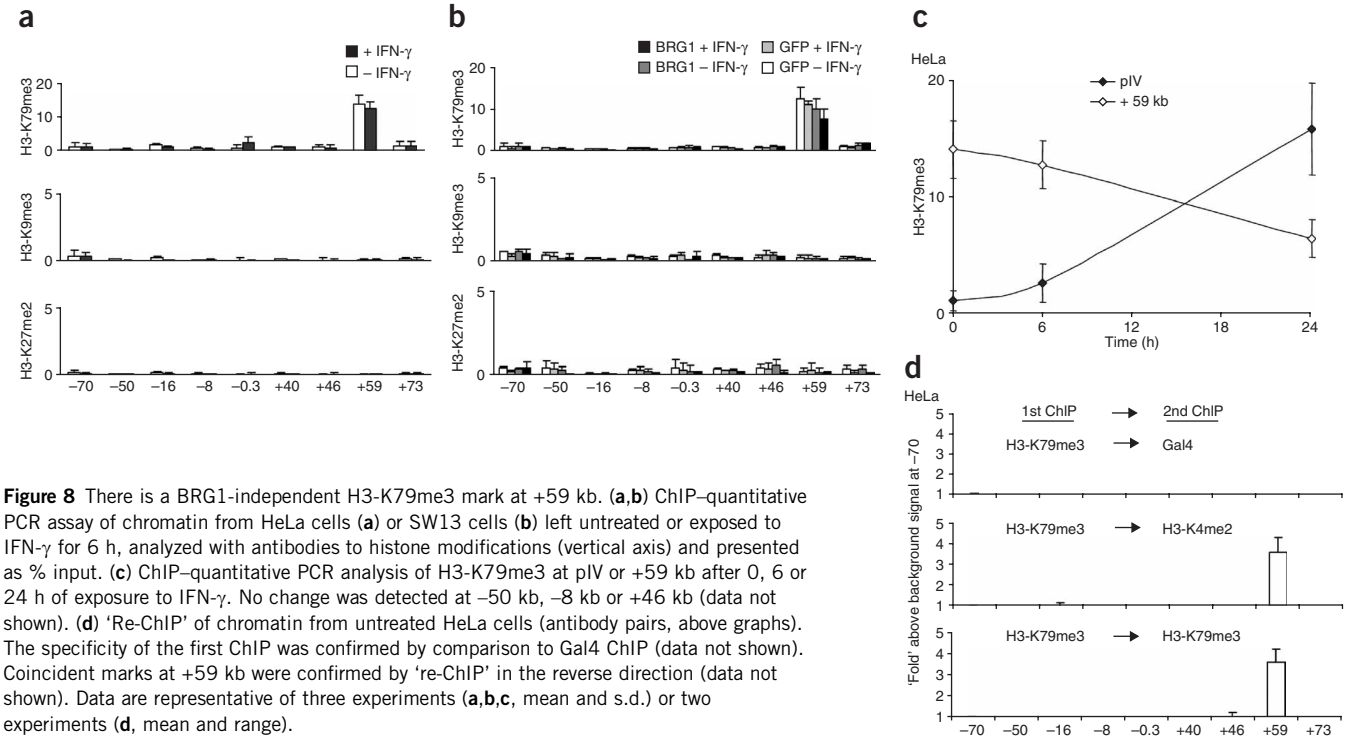

Figure 8 There is a BRG1-independent H3-K79me3 mark at +59 kb. (**a**,**b**) ChIP–quantitative PCR assay of chromatin from HeLa cells (**a**) or SW13 cells (**b**) left untreated or exposed to IFN-γ for 6 h, analyzed with antibodies to histone modifications (vertical axis) and presented as % input. (**c**) ChIP–quantitative PCR analysis of H3-K79me3 at pIV or +59 kb after 0, 6 or 24 h of exposure to IFN-γ. No change was detected at –50 kb, –8 kb or +46 kb (data not shown). (**d**) 're-ChIP' of chromatin from untreated HeLa cells (antibody pairs, above graphs). The specificity of the first ChIP was confirmed by comparison to Gal4 ChIP (data not shown). Coincident marks at +59 kb were confirmed by 're-ChIP' in the reverse direction (data not shown). Data are representative of three experiments (**a**,**b**,**c**, mean and s.d.) or two experiments (**d**, mean and range).

(**Figs. 2** and **5**), although we found transcription factor binding and histone modifications only in HeLa cells (**Figs. 1d** and **3** and **Supplementary Table 1**). The reason for the latter cell-type difference is unclear, as the sequence of HeLa, SW13 or BAC DNA in this region is identical (data not shown), but it could relate to the strength of looping, which is higher in HeLa cells. Whatever the reason, the data reported above show that remote elements are critical for IFN-γ responsiveness, as, like BRG1 absence, deletion of any one of five but not two irrelevant sites silenced *CIITA*.

BRG1-independent H3-K79me3 at +59 kb

The BRG1 dependency of *CIITA* pIV was relieved when flanking sequences were removed (**Fig. 1a**,**b**), which indicated that BRG1 may be needed to overcome active repression by remote sites. In a first step toward identifying putative negative influences, we searched for repressive chromatin 'signatures' at many sites across the *CIITA* locus. We assessed three modifications, H3-K9me3, H3-K27me2 and H3-K79me3, which, as shown by a genome-wide study, are associated with silent loci[43]. We detected no H3-K9me3 or H3-K27me2 at 0 or 6 h after IFN-γ, but we did detect a constitutive H3-K79me3 mark at +59 kb (**Fig. 8a**,**b**). Consistent with the idea that BRG1 may act downstream to temper its negative influence, we noted H3-K79me3 in both BRG1-expressing HeLa cells and BRG1-deficient or BRG1-expressing SW13 cells, with or without IFN-γ. This mark was specific, as it was absent from the other four enhancers, pIV and three irrelevant control *CIITA* sites (**Fig. 8a**,**b**). We also analyzed H3-K79me3 at a subset of sites at 24 h and detected 14.5-fold induction at pIV, which was accompanied by a modest drop by 50% at +59 kb (**Fig. 8c**). The substantial increase at pIV occurs at a time when the RNA polymerase II enhanceosome, containing the transcription factors STAT1, IRF1, USF1 and Myc, is being disassembled[34]. Thus, H3-K79me3 at remote or proximal sites correlates with *CIITA* repression. The constitutive BRG1-independent H3-K79me3 mark at +59 kb (**Fig. 8a**,**b**) coincides with a BRG1-independent, constitutive, H3-K4me2 activating 'signature' (**Fig. 3b**). Consecutive ChIP with antibodies to H3-K4me2, then to H3-K79me3, or vice versa, showed that both marks coexisted on the same allele (**Fig. 8d** and data not shown). These concurrent marks with potentially opposite functions are reminiscent of the bivalent elements found in embryonic stem cells at developmentally important genes poised for lineage-dependent activation or permanent silencing[37,44].

DISCUSSION

BRG1 is required for the induction of many ISGs, and the promoter is believed to be sufficient to confer this dependency[9,22,30,32]. Our hypothesis that BRG1 acts through remote *CIITA* elements arose from the observation that IFN-γ induction of endogenous pIV is BRG1 dependent, whereas induction of isolated pIV, lacking distal sites, is BRG1 independent. The use of a replicating (properly chromatin-associated) vector and extension of the 5′ segment to 8 kb did not confer BRG1 dependency. However, after mapping extensive IFN-γ-induced events at remote sites across a domain of about 110 kb, we generated a large BAC vector that showed BRG1-dependent induction. Although the possibility is difficult to exclude formally, it seems unlikely that the BRG1 dependency of long but not short *CIITA* reporters is vector related, as the same backbone used for short reporters here has demonstrated the BRG1 dependency of other isolated ISG promoters[22,32]. More notably, remote elements bind BRG1 and show BRG1-dependent activator recruitment, histone modifications, accessibility and looping, which together provide a compelling case that distal elements are critical for conferring BRG1 dependency. BRG1 also binds pIV (refs. 9,30 and reported here), so it may have direct effects on the promoter; however, regardless of whether that is true, pIV was insufficient to confer BRG1 dependency. Like BRG1, five remote enhancers were each critical for *CIITA* induction. Alleviation of this dependency on either BRG1 or the newly identified enhancers in short reporters supports the idea of as-yet-unidentified remote silencers that actively block *CIITA* induction (discussed further below). Previous models of *CIITA* induction have focused on the recruitment of STAT1 and IRF1 to proximal elements. Our results have shown complex interaction among many BRG1-dependent distal sites. Remote binding of STAT1 around ISGs has been described[36,45–48], but the functional relevance has remained unclear. Here we have provided proof that remote events are essential for IFN-γ-signaling and have detailed the cascade that triggers *CIITA* induction.

The new model of *CIITA* induction includes many steps. In the basal state and independently of BRG1, the site at +59 kb, which has H3-K4me2 and H3-K79me3 modifications, loops and contacts the site at –50 kb, and the element at –8 kb bridges this complex to pIV. Different pairs of contacts may occur separately at different alleles, but whether or not that occurs, our data have shown extensive BRG1-independent looping in the basal state. BRG1 did not induce more looping but was recruited to the site at –50 kb and triggered a second H3-K4me2 mark. Of note, BRG1 can bind and/or act together with histone methyltransferases[39,40]. BAC studies have proven the functional relevance of the sites at +59 kb and –50 kb; thus, BRG1-independent H3-K4me2 at +59 kb may prime the locus for BRG1 recruitment, and BRG1-dependent H3-K4me2 at –50 kb may make it poised for induction. In this poised state, BRG1 may temper repressive effects, potentially involving the H3-K79me3-marked site at +59 kb. Once *CIITA* is primed, IFN-γ triggers many events, including recruitment of STAT1 and IRF1 to remote sites, histone acetylation, chromatin remodeling, more looping, recruitment of RNA polymerase II and transcription. Notably, this multifactorial cascade is halted in the absence of BRG1.

The potential repressive function of H3-K79me3 at *CIITA* is only speculative. H3-K79me3 is commonly associated with remote silent loci[43], and K79 methylation is needed to maintain androgen target genes in a repressed state[49]. However, a study has shown that H3-K79me3 is common near active transcriptional start sites, although its removal does not affect expression of these targets[50]. Of note, we also found that enhanceosome disassembly at pIV correlated with H3-K79me3 induction, which further indicated that, as at androgen target genes[49], K79 methylation may negatively regulate *CIITA*. A future goal will be to define the mechanism underlying K79 methylation and its relevance.

SWI-SNF can link distant nucleosomes on arrays formed *in vitro*[29]. At the *CIITA* locus, the addition of BRG1 did not trigger looping, but it was necessary for IFN-γ-induced looping. BRG1 may facilitate IFN-γ-induced looping either indirectly, by enhancing the recruitment of factors that mediate long-range interactions, or directly, through interaction with activators at other sites. The idea of a potential direct function is supported by the fact that BRG1 binds STAT and IRF proteins[14,31].

Why does the removal of BRG1 or deletion of one enhancer block the action of all remote enhancers? Perhaps the enhancers function as a single cooperative unit; thus, loss of BRG1 or enhancer disrupts this cooperation, resulting in passive repression due to failure to engage the entire unit. Alternatively, *CIITA* silencing may be actively mediated by repressors. Indeed, as noted earlier, BRG1 or enhancer dependency is alleviated in short reporters, which suggests that these vectors lack

remote silencers. This model is reminiscent of the antagonism between Brahma, the drosophila BRG1 ortholog and the Polycomb group repressors[51]. Moreover, trichostatin A, a histone deacetylase inhibitor, restores the IFN-γ responsiveness of *CIITA* in BRG1-deficient cells[52]. Trichostatin A sometimes derepresses expression of the *BRG1*-related gene *SMARCA2* (also called BRM), but this is not the case in our clone of SW13 cells[52]. Thus, histone deacetylases may actively repress *CIITA* in the absence of BRG1. In summary, our extensive biochemical and genetic analyses have shown many newly identified BRG1-dependent remote elements that regulate the basal and IFN-γ activated status of the *CIITA* locus. Genetic or epigenetic effects at these elements could be a previously unknown mechanism underlying one of the many diseases already linked to altered *CIITA* expression[1–3].

METHODS

Cell culture and adenoviruses. Human cervical carcinoma HeLa-ini1-11 (HeLa) and adenocarcinoma SW13 cells were grown as described[9]. Cells were treated with human IFN-γ (0.1 μg/ml; BioSource International). Virus was produced and SW13 cells were transduced as described[9]. The amount of virus was 'titrated' so that BRG1 expression was equivalent to that in HeLa cells[9].

Plasmid construction and reporter assays. Details of plasmid construction are in the **Supplementary Methods**. Cells were transfected with Lipofectamine (Invitrogen), Lipofectin (Invitrogen) or calcium phosphate. In transient assays, 0.01 μg renilla luciferase plasmid was included to normalize transfection efficiency. Luciferase assays were done as described[9].

RNA quantification. RNA was isolated, reverse-transcribed and analyzed by quantitative PCR and values were normalized to those of β-actin as described[9]. Primers are in **Supplementary Table 3** online.

ChIP on tiled genome arrays, ChIP–quantitative PCR and 're-ChIP'. Details of primers and antibodies used in ChIP assays are in **Supplementary Tables 3** and **4** online, respectively. Crosslinked chromatin was sonicated to an average size of about 500 base pairs and was incubated with antibody to STAT1 (anti-STAT1), anti-IRF1, anti-H3ac or anti-H4ac; bound fragments were purified by ChIP as described[9], amplified by ligation-mediated PCR (discussed below) and labeled, then hybridized to custom-built genomic tiling arrays (Nimblegen). Hybridization intensities were normalized to internal standards and values from quadruplicate spots were averaged. Significantly different intensities between ChIP DNA and input DNA samples in three biological replicates ($P < 0.0001$) were determined with the Wilcoxon rank-sum test. Peaks representing significantly enriched DNA regions ($P < 0.0001$) where the ratio of ChIP to input DNA was 1.5-fold or more were visualized with the University of California at Santa Cruz Human (*Homo sapiens*) Genome Browser (PhastCons) and are plotted on a $\log_2$ scale. Peaks in a sliding window of 500 base pairs were merged with an in-house Perl script pipeline. ChIP–quantitative PCR was done as described, and in all cases, the low background signal obtained with an irrelevant antibody to the yeast transcriptional activator Gal4 was subtracted[9]. 'Re-ChIP' (sequential ChIP with two different antibodies) was done as described[53].

Ligation-mediated PCR. The annealed linker primers oJW102 (5′-GCG GTGACCCGGGAGATCTGAATTC-3′) and oJW103 (5′-GAATTCAGATC-3′) were used for ligation-mediated PCR. Blunt ends were created in chromatin DNA by incubation for 45 min to about 60 min at 37 °C with T4 DNA polymerase, followed by purification with the Qiaquick PCR purification kit. Blunted chromatin DNA was ligated to the linker at 16 °C overnight and was purified. Sample were amplified in the following conditions: one cycle at 55 °C for 2 min, 72 °C for 5 min and 95 °C for 2 min, followed by 20 cycles at 95 °C for 30 s, 55 °C for 30 s and 72 °C for 1 min and one cycle at 72 °C for 4 min. DNA was finally purified with Qiaquick.

Chromosome conformation capture. This assay was done as described[38] with minor modifications (details, **Supplementary Methods**; primers, **Supplementary Table 5** online).

DNase I accessibility. Nuclei were prepared and digested with DNase I as described[30] (primers, **Supplementary Table 3**).

BAC manipulation. Bacteria carrying the human BAC CTD-2577P18, which contains 194-kb region spanning the *CIITA* locus, were obtained from Invitrogen. Recombination-mediated genetic engineering was used for growth and manipulation of the BACs as described[42]. Details of the creation of BAC-*CIITA* and its derivatives, the generation of stable SW13 clones and the quantification of BAC DNA are in the **Supplementary Methods**. Oligonucleotides and BAC quantification primers are in **Supplementary Tables 6** and **7** online, respectively.

Statistical analysis. Significance was assessed by analysis of variance with an *ad hoc* Fisher's least significant difference test to adjust for multiple tests.

Accession codes. UCSD-Nature Signaling Gateway (http://www.signaling-gateway.org): A000657 and A001238; GEO: microarray data, GSE10206.

Note: Supplementary information is available on the Nature Immunology website.

ACKNOWLEDGMENTS

We thank L. Zeng for technical assistance; D. Torti for help with statistics; P. Farnham for protocols and advice for ChIP on tiled genome arrays; R Métivier for protocols and advice for 're-ChIP'; N. Copeland (National Cancer Institute) for reagents and advice for recombination-mediated genetic engineering; and H. Lipps (University Witten/Herdecke), J.F. Piskurich (Mercer University School of Medicine) and K. Zhao (National Institutes of Health) for plasmids. Supported by the National Cancer Institute of Canada with funds from the Canadian Cancer Society and from the Krembil Foundation, Ontario Graduate Studentships (Z.N.), the Vision Science Research Program (Z.N.), the Frank Fletcher Memorial Fund (Z.N.), Dr. R. Dittakavi & Dr. P. Rao Graduate Award (Z.N.) and the Krembil Foundation (M.A.E.H.).

AUTHOR CONTRIBUTIONS

Z.N. and M.A.E.H designed and did experiments, analyzed data and wrote the manuscript; Z.X. analyzed data; T.Y. did experiments; and R.B. designed and supervised the research, analyzed data and wrote the manuscript.

Published online at http://www.nature.com/natureimmunology/
Reprints and permissions information is available online at http://npg.nature.com/reprintsandpermissions/

1. Wright, K.L. & Ting, J.P. Epigenetic regulation of MHC-II and CIITA genes. *Trends Immunol.* **27**, 405–412 (2006).
2. Swanberg, M. *et al.* MHC2TA is associated with differential MHC molecule expression and susceptibility to rheumatoid arthritis, multiple sclerosis and myocardial infarction. *Nat. Genet.* **37**, 486–494 (2005).
3. Holling, T.M., van Eggermond, M.C., Jager, M.J. & van den Elsen, P.J. Epigenetic silencing of MHC2TA transcription in cancer. *Biochem. Pharmacol.* **72**, 1570–1576 (2006).
4. Dunn, G.P., Koebel, C.M. & Schreiber, R.D. Interferons, immunity and cancer immunoediting. *Nat. Rev. Immunol.* **6**, 836–848 (2006).
5. Maher, S.G., Romero-Weaver, A.L., Scarzello, A.J. & Gamero, A.M. Interferon: cellular executioner or white knight? *Curr. Med. Chem.* **14**, 1279–1289 (2007).
6. Ullrich, E. *et al.* Therapy-induced tumor immunosurveillance involves IFN-producing killer dendritic cells. *Cancer Res.* **67**, 851–853 (2007).
7. Muhlethaler-Mottet, A., Di Berardino, W., Otten, L.A. & Mach, B. Activation of the MHC class II transactivator CIITA by interferon-γ requires cooperative interaction between Stat1 and USF-1. *Immunity* **8**, 157–166 (1998).
8. Morris, A.C., Beresford, G.W., Mooney, M.R. & Boss, J.M. Kinetics of a gamma interferon response: expression and assembly of CIITA promoter IV and inhibition by methylation. *Mol. Cell. Biol.* **22**, 4781–4791 (2002).
9. Ni, Z. *et al.* Apical role for BRG1 in cytokine-induced promoter assembly. *Proc. Natl. Acad. Sci. USA* **102**, 14611–14616 (2005).
10. Muhlethaler-Mottet, A., Otten, L.A., Steimle, V. & Mach, B. Expression of MHC class II molecules in different cellular and functional compartments is controlled by differential usage of multiple promoters of the transactivator CIITA. *EMBO J.* **16**, 2851–2860 (1997).
11. van der Stoep, N. *et al.* Constitutive and IFNγ-induced activation of MHC2TA promoter type III in human melanoma cell lines is governed by separate regulatory elements within the PIII upstream regulatory region. *Mol. Immunol.* **44**, 2036–2046 (2007).
12. Piskurich, J.F., Linhoff, M.W., Wang, Y. & Ting, J.P. Two distinct gamma interferon-inducible promoters of the major histocompatibility complex class II transactivator gene are differentially regulated by STAT1, interferon regulatory factor 1, and transforming growth factor beta. *Mol. Cell. Biol.* **19**, 431–440 (1999).
13. Chi, T. A BAF-centred view of the immune system. *Nat. Rev. Immunol.* **4**, 965–977 (2004).

14. Kadam, S. & Emerson, B.M. Transcriptional specificity of human SWI/SNF BRG1 and BRM chromatin remodeling complexes. *Mol. Cell* **11**, 377–389 (2003).
15. Muchardt, C. & Yaniv, M. When the SWI/SNF complex remodels…the cell cycle. *Oncogene* **20**, 3067–3075 (2001).
16. Trotter, K.W. & Archer, T.K. Nuclear receptors and chromatin remodeling machinery. *Mol. Cell. Endocrinol.* **265–266**, 162–167 (2007).
17. Agalioti, T., Chen, G. & Thanos, D. Deciphering the transcriptional histone acetylation code for a human gene. *Cell* **111**, 381–392 (2002).
18. Salma, N., Xiao, H., Mueller, E. & Imbalzano, A.N. Temporal recruitment of transcription factors and SWI/SNF chromatin-remodeling enzymes during adipogenic induction of the peroxisome proliferator-activated receptor γ nuclear hormone receptor. *Mol. Cell. Biol.* **24**, 4651–4663 (2004).
19. Armstrong, J.A., Bieker, J.J. & Emerson, B.M.A. SWI/SNF-related chromatin remodeling complex, E-RC1, is required for tissue-specific transcriptional regulation by EKLF in vitro. *Cell* **95**, 93–104 (1998).
20. Fryer, C.J. & Archer, T.K. Chromatin remodelling by the glucocorticoid receptor requires the BRG1 complex. *Nature* **393**, 88–91 (1998).
21. Liu, R. *et al.* Regulation of CSF1 promoter by the SWI/SNF-like BAF complex. *Cell* **106**, 309–318 (2001).
22. Liu, H., Kang, H., Liu, R., Chen, X. & Zhao, K. Maximal induction of a subset of interferon target genes requires the chromatin-remodeling activity of the BAF complex. *Mol. Cell. Biol.* **22**, 6471–6479 (2002).
23. Chi, T.H. *et al.* Reciprocal regulation of CD4/CD8 expression by SWI/SNF-like BAF complexes. *Nature* **418**, 195–199 (2002).
24. Cai, S., Lee, C.C. & Kohwi-Shigematsu, T. SATB1 packages densely looped, transcriptionally active chromatin for coordinated expression of cytokine genes. *Nat. Genet.* **38**, 1278–1288 (2006).
25. Im, H. *et al.* Chromatin domain activation via GATA-1 utilization of a small subset of dispersed GATA motifs within a broad chromosomal region. *Proc. Natl. Acad. Sci. USA* **102**, 17065–17070 (2005).
26. O'Neill, D. *et al.* Tissue-specific and developmental stage-specific DNA binding by a mammalian SWI/SNF complex associated with human fetal-to-adult globin gene switching. *Proc. Natl. Acad. Sci. USA* **96**, 349–354 (1999).
27. Bultman, S.J., Gebuhr, T.C. & Magnuson, T.A. Brg1 mutation that uncouples ATPase activity from chromatin remodeling reveals an essential role for SWI/SNF-related complexes in β-globin expression and erythroid development. *Genes Dev.* **19**, 2849–2861 (2005).
28. Kim, S.I., Bultman, S.J., Jing, H., Blobel, G.A. & Bresnick, E.H. Dissecting molecular steps in chromatin domain activation during hematopoietic differentiation. *Mol. Cell. Biol.* **27**, 4551–4565 (2007).
29. Bazett-Jones, D.P., Cote, J., Landel, C.C., Peterson, C.L. & Workman, J.L. The SWI/SNF complex creates loop domains in DNA and polynucleosome arrays and can disrupt DNA-histone contacts within these domains. *Mol. Cell. Biol.* **19**, 1470–1478 (1999).
30. Pattenden, S.G., Klose, R., Karaskov, E. & Bremner, R. Interferon-gamma-induced chromatin remodeling at the CIITA locus is BRG1 dependent. *EMBO J.* **21**, 1978–1986 (2002).
31. Huang, M. *et al.* Chromatin-remodelling factor BRG1 selectively activates a subset of interferon-α-inducible genes. *Nat. Cell Biol.* **4**, 774–781 (2002).
32. Cui, K. *et al.* The chromatin-remodeling BAF complex mediates cellular antiviral activities by promoter priming. *Mol. Cell. Biol.* **24**, 4476–4486 (2004).
33. Yan, Z. *et al.* PBAF chromatin-remodeling complex requires a novel specificity subunit, BAF200, to regulate expression of selective interferon-responsive genes. *Genes Dev.* **19**, 1662–1667 (2005).
34. Ni, Z. & Bremner, R. Brahma-related gene 1-dependent STAT3 recruitment at IL-6-inducible genes. *J. Immunol.* **178**, 345–351 (2007).
35. Bernstein, B.E. *et al.* Genomic maps and comparative analysis of histone modifications in human and mouse. *Cell* **120**, 169–181 (2005).
36. Heintzman, N.D. *et al.* Distinct and predictive chromatin signatures of transcriptional promoters and enhancers in the human genome. *Nat. Genet.* **39**, 311–318 (2007).
37. Bernstein, B.E., Meissner, A. & Lander, E.S. The mammalian epigenome. *Cell* **128**, 669–681 (2007).
38. Dekker, J., Rippe, K., Dekker, M. & Kleckner, N. Capturing chromosome conformation. *Science* **295**, 1306–1311 (2002).
39. Bultman, S.J. *et al.* Maternal BRG1 regulates zygotic genome activation in the mouse. *Genes Dev.* **20**, 1744–1754 (2006).
40. Nakamura, T. *et al.* ALL-1 is a histone methyltransferase that assembles a supercomplex of proteins involved in transcriptional regulation. *Mol. Cell* **10**, 1119–1128 (2002).
41. Baiker, A. *et al.* Mitotic stability of an episomal vector containing a human scaffold/matrix-attached region is provided by association with nuclear matrix. *Nat. Cell Biol.* **2**, 182–184 (2000).
42. Warming, S., Costantino, N., Court, D.L., Jenkins, N.A. & Copeland, N.G. Simple and highly efficient BAC recombineering using galK selection. *Nucleic Acids Res.* **33**, e36 (2005).
43. Barski, A. *et al.* High-resolution profiling of histone methylations in the human genome. *Cell* **129**, 823–837 (2007).
44. Azuara, V. *et al.* Chromatin signatures of pluripotent cell lines. *Nat. Cell Biol.* **8**, 532–538 (2006).
45. Hartman, S.E. *et al.* Global changes in STAT target selection and transcription regulation upon interferon treatments. *Genes Dev.* **19**, 2953–2968 (2005).
46. Bhinge, A.A., Kim, J., Euskirchen, G.M., Snyder, M. & Iyer, V.R. Mapping the chromosomal targets of STAT1 by sequence tag analysis of genomic enrichment (STAGE). *Genome Res.* **17**, 910–916 (2007).
47. Robertson, G. *et al.* Genome-wide profiles of STAT1 DNA association using chromatin immunoprecipitation and massively parallel sequencing. *Nat. Methods* **4**, 651–657 (2007).
48. Christova, R. *et al.* P-STAT1 mediates higher-order chromatin remodelling of the human MHC in response to IFNγ. *J. Cell. Sci.* **120**, 3262–3270 (2007).
49. Zhang, W. *et al.* Aldosterone-sensitive repression of ENaCα transcription by a histone H3 lysine-79 methyltransferase. *Am. J. Physiol. Cell Physiol.* **290**, C936–C946 (2006).
50. Steger, D.J. *et al.* DOT1L/KMT4 recruitment and H3K79 methylation are ubiquitously coupled with gene transcription in mammalian cells. *Mol Cell Biol* (2008).
51. Tamkun, J.W. *et al.* brahma: a regulator of *Drosophila* homeotic genes structurally related to the yeast transcriptional activator SNF2/SWI2. *Cell* **68**, 561–572 (1992).
52. Pattenden, S. *Analysis of chromatin remodeling in an IFN-γ responsive system.* Thesis, Univ. Toronto (2003).
53. Reid, G. *et al.* Cyclic, proteasome-mediated turnover of unliganded and liganded ERα on responsive promoters is an integral feature of estrogen signaling. *Mol. Cell* **11**, 695–707 (2003).

SUPPLEMENTAL DATA

BRG1 coordinates *CIITA* induction through multiple inter-dependent remote enhancers

Zuyao Ni, Mohamed Abou El Hassan, Zhaodong Xu, Tao Yu, and Rod Bremner

CONTENTS:

Page 2…Supplemental Figures:

Page 2…Figure S1: IFN-γ triggers looping at the *CIITA* locus

Page 3…Figure S2: Summary of events at *CIITA* in two cell types

Page 4… Figure S3: Looping is not a non-specific result of proximity

Page 4…Figure S4: BRG1 dependent and independent chromatin looping

Page 5… Figure S5: Distal elements alter promoter activity

Page 6… Figure S6: Recombineering strategy to generate the BAC-*CIITA* reporter and derivatives

Page 7…Supplemental Tables:

Page 7… Table S1: Summary of key events at the *CIITA* locus in HeLa and SW13 cells

Page 8… Table S2: Regression analysis: looping is not a non-specific consequence of proximity

Page 9… Table S3: qPCR Primers

Page 10…Table S4: Antibodies

Page 11…Table S5: 3C Primers

Page 12…Table S6: Recombineering oligonucleotides

Page 12…Table S7: BAC quantification primers

Page 13…Supplemental experimental procedures

Page 19…Supplemental References

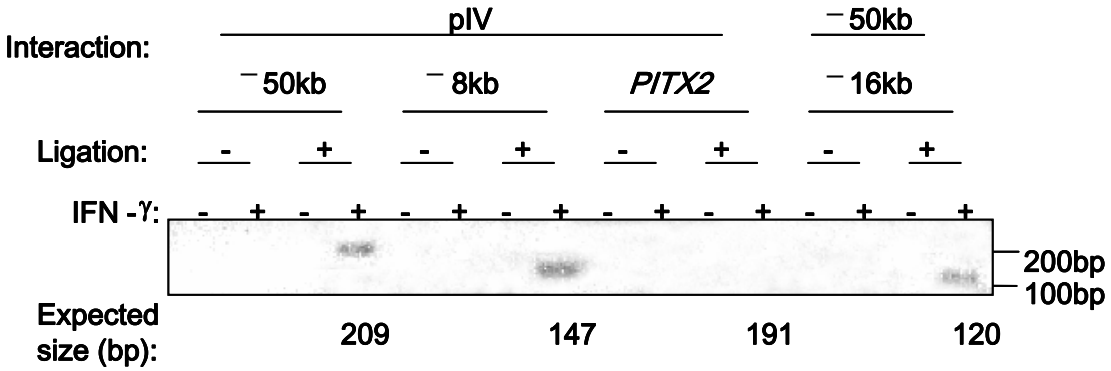

Fig S1. IFN-γ triggers looping at the *CIITA* locus. 3C was performed using chromatin from HeLa cells to assess interaction between pIV and the -50 or -8 kb *CIITA* elements or the irrelevant *PITX2* locus, as well as between the -50 and -16 kb *CIITA* sites. The results were analyzed by gel-based PCR. Results are representative of at least three experiments.

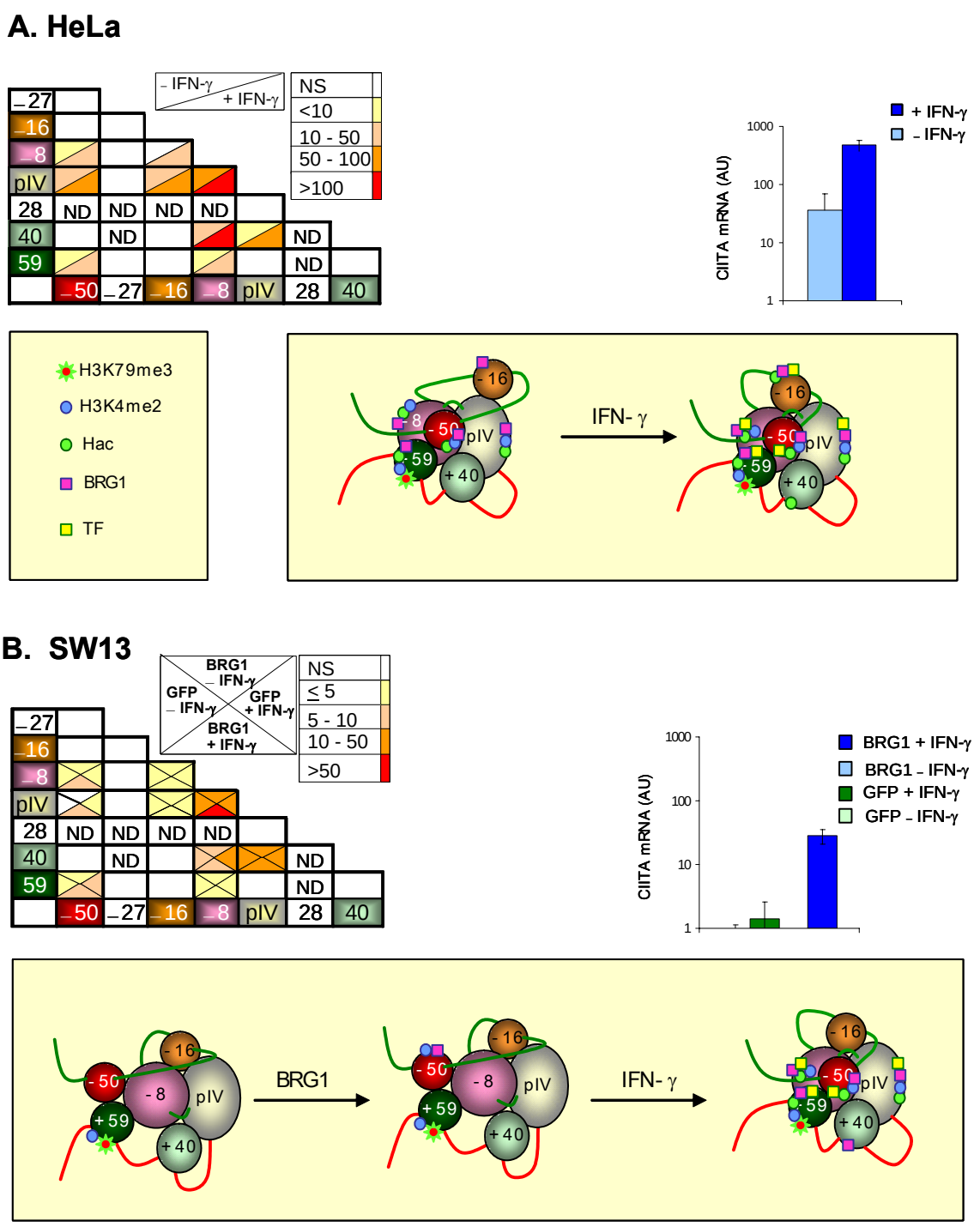

Fig S2. Summary of events at *CIITA* in two cell types. The triangular matrices indicate the strength of interaction between 7 sites (five remote enhancers, pIV, and two controls) using a heat map ranging from white (no interaction) to red (strong binding) (3C data from **Fig 2, 5**). ND: not determined. The schematic diagrams visually depict looping events, as well as the histone modifications (circles) or factors (squares, TF: STAT1 and/or IRF1) associated with each element (ChIP data from **Fig 1, 3, 8**). The red and green lines represent DNA up or downstream of pIV, respectively. The graphs also show the level of *CIITA* mRNA in each cell type (log scale).

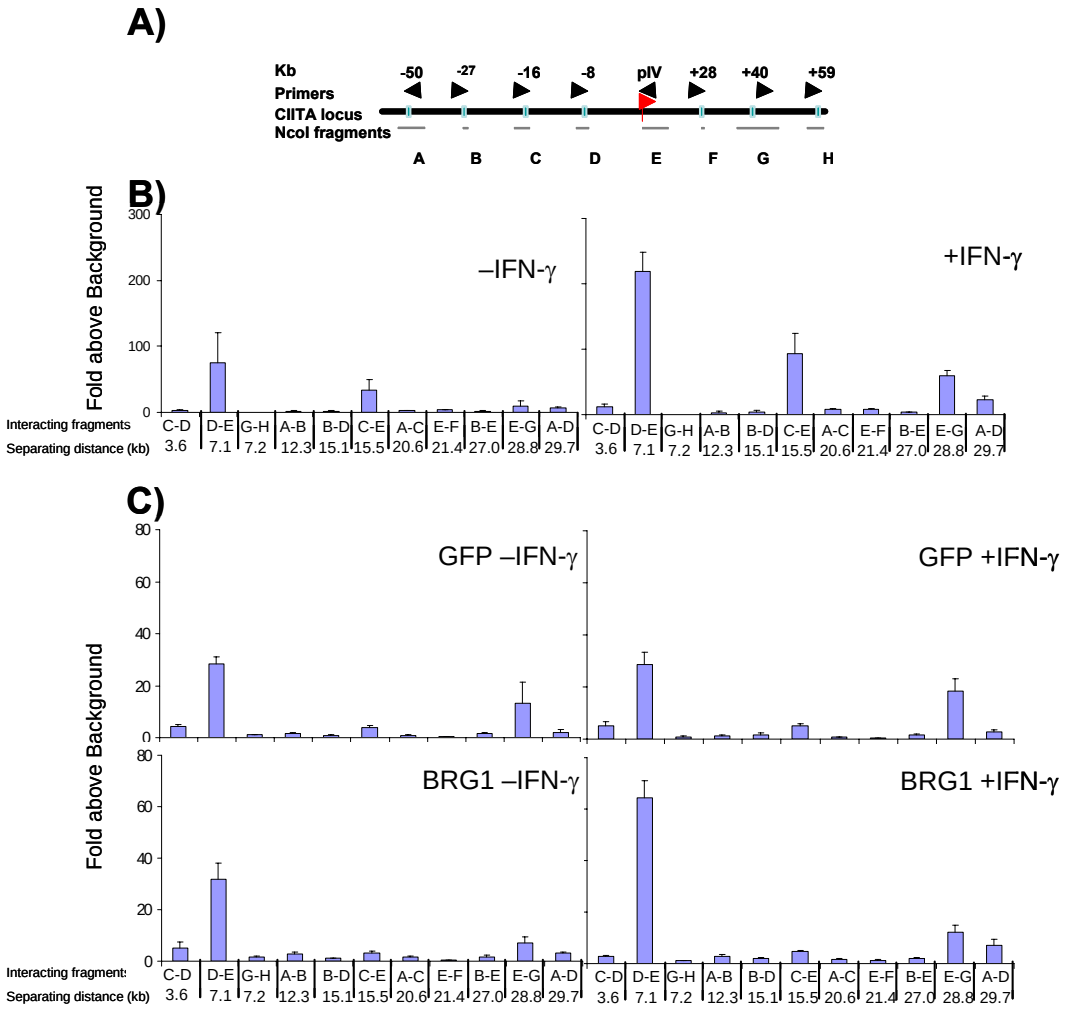

Fig S3. Looping is not a non-specific result of proximity. (a) A schematic diagram of the *CIITA* locus. The diagram is laid out as in Fig 2. **(b, c)** The looping frequency as a function of distance between fragments in HeLa **(b)** and SW13 **(c)** cells treated as indicated.

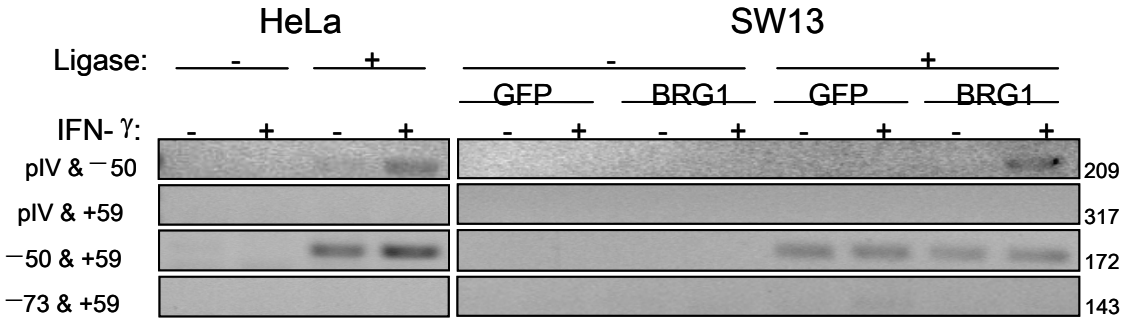

Fig S4. BRG1 dependent and independent chromatin looping. 3C assays were performed on chromatin from HeLa cells (left panel), or SW13 cells expressing GFP or BRG1 (right panel), left untreated or exposed to IFN-γ for 6 hrs. The results were analyzed by gel-based PCR. Interactions tested are indicated on the left and the size in bp of expected PCR product is shown on the right. The -73 kb site is an inactive chromatin region.

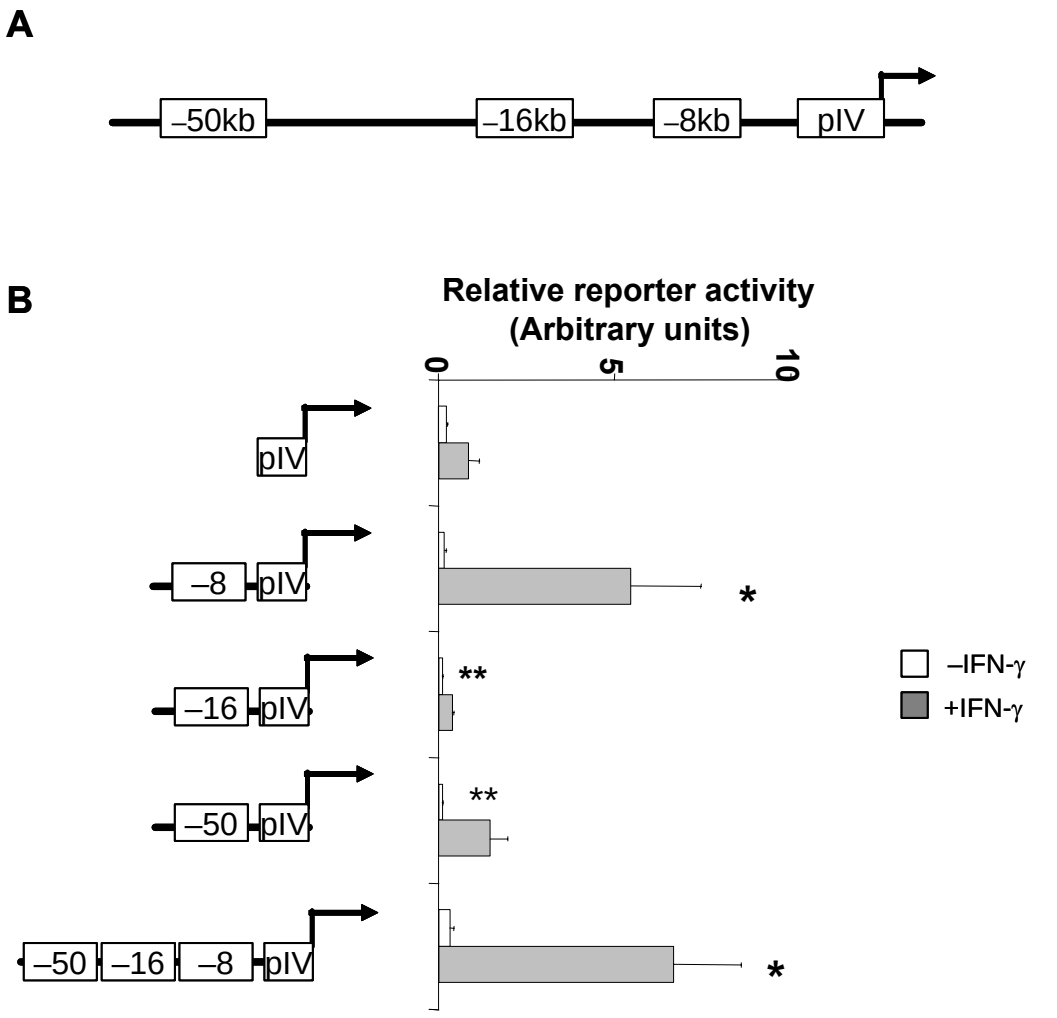

Fig. S5. Distal elements alter promoter activity. (**a**). A schematic diagram of ChIP-chip flagged peaks upstream of *CIITA* pIV. (**b**). Luc activity. Selected sequences were cloned individually or in combination upstream of the *CIITA* pIV-Luc cassette in the pREP4 plasmids. Luc activity was measured in HeLa cells transfected with the indicated plasmids, together with a Renilla plasmid to control for transfection efficiency. Results are representative of three experiments (mean +/-SD). Significant changes ($P < 0.05$) relative to the basal (**) or IFN-γ-induced (*) activity of the pIV promoter vector.

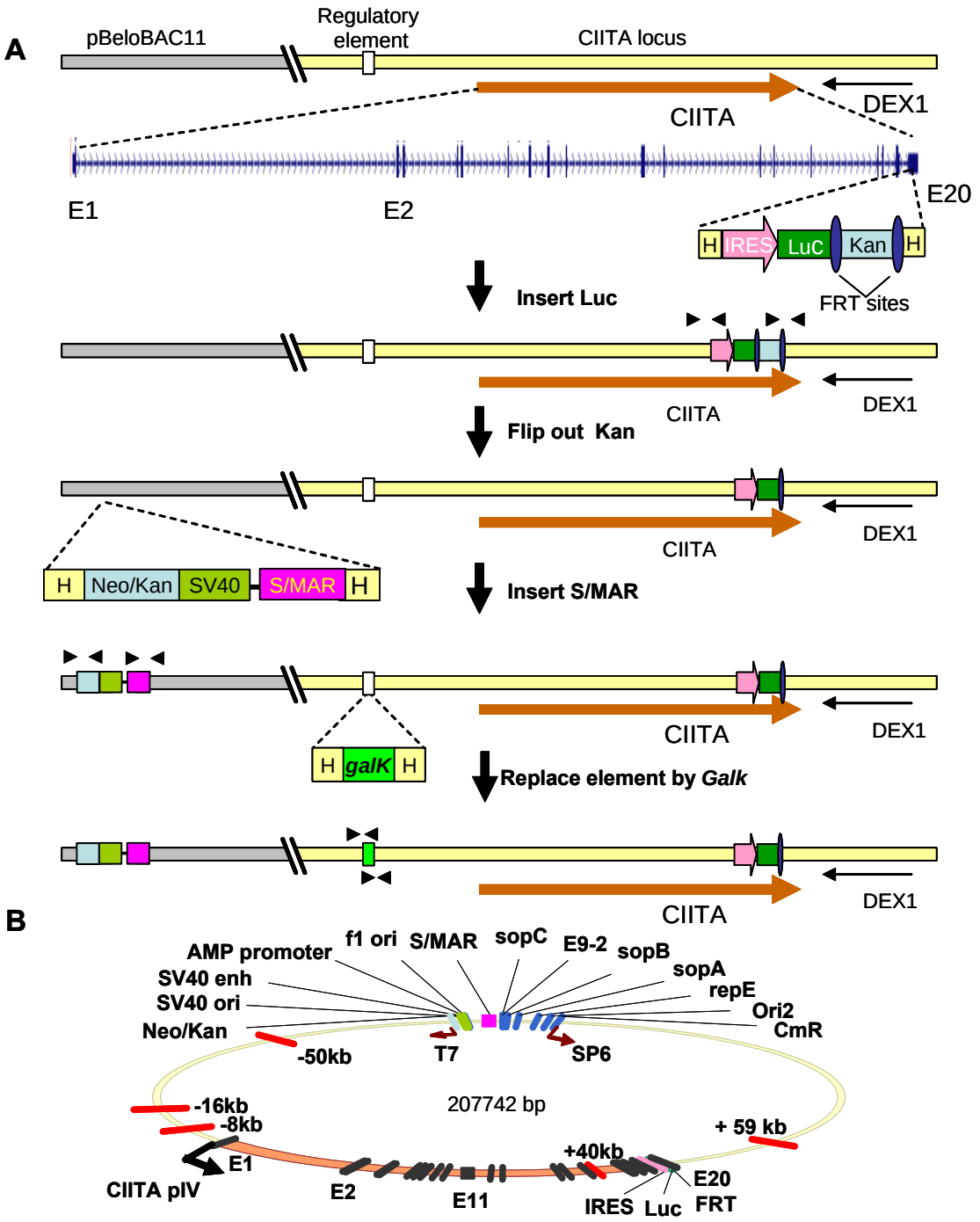

Fig S6. Strategy to generate the BAC-*CIITA* reporter and derivatives. (**a**). Recombineering steps used to generate the BAC-*CIITA* reporter and replacement mutants. H: homologous arms. The paired arrows represent primer pairs used to verify the inserted elements. (**b**). The BAC-*CIITA* reporter vector. Brown box: *CIITA* gene body; black bars: *CIITA* exons; red bars: remote regulatory elements; blue bars: BAC elements.

Table S1: Summary of key events at the *CIITA* locus in HeLa and SW13 cells

Recruitment or modification	Cells	IFN-γ (hrs)	Element					
			-50	-16	-8	pIV	+40	+59
BRG1	SW13 GFP	0	-	-	-	-	-	-
		6	-	-	-	-	-	-
	SW13 BRG1	0	++	-	-	++	++	+
		6	+++	-	+++	+++	+++	+++
	HeLa	0	+	+	++	+	-	-
		6	++	++	++	++	-	++
STAT1	SW13 GFP	0	-	-	-	-	-	-
		6	-	-	-	-	-	-
	SW13 BRG1	0	-	-	-	-	-	-
		6	+++	-	++	+++	-	-
	HeLa	0	-	-	-	-	-	-
		6	+	-	++	++		-
IRF1	SW13 GFP	0	-	-	-	-	-	-
		6	-	-	-	-	-	-
	SW13 BRG1	0	-	-	-	-	-	-
		6	-	-	-	+++	-	++
	HeLa	0	-	-	-	-	-	-
		6	++	++	+++	+++	-	+++
H3ac	SW13 GFP	0	-	-	-	-	-	-
		6	-	-	-	-	-	-
	SW13 BRG1	0	-	-	-	-	-	-
		6	+	-	-	+	-	++
	HeLa	0	+	-	-	+	-	-
		6	++	+	+	++	+	+
H4ac	SW13 GFP	0	-	-	-	-	-	-
		6	+	-	-	-	-	-
	SW13 BRG1	0	-	-	-	-	-	-
		6	+++	-	++	++	-	-
	HeLa	0	+++	+	++	++	-	-
		6	+++	++	+++	+++	++	-
H3K4me2	SW13 GFP	0	-	-	-	-	-	++
		6	-	-	-	+	-	++
	SW13 BRG1	0	++	-	+	+	-	++
		6	++	-	+	++	-	++
	HeLa	0	+++	-	++	+++	-	++
		6	+++	-	++	+++	-	++

A minus sign indicates no significant difference between the ChIP signal at that element and background signal at -70 kb. Plus signs indicate both a significant difference ($P < 0.01$) and an increase over background at -70 kb of +: >5 and ≤10 fold, ++: >10 and ≤30 fold; +++: >30 fold.

Table S2: Regression analysis: looping is not a non-specific consequence of proximity

	Correlation coefficient (R^2)	
Group	**Linear regression**	**Nonlinear regression**
HeLa –IFN-γ	0.09	0.10
HeLa +IFN-γ	0.08	0.08
SW13 +GFP –IFN-γ	0.08	0.12
SW13 +BRG1 –IFN-γ	0.09	0.15
SW13 +GFP +IFN-γ	0.04	0.07
SW13 +BRG1 +IFN-γ	0.07	0.11

21 interactions were assessed among 8 fragments at *CIITA*. The frequency of each of the interactions was plotted against distance between each fragment and both linear and non-linear regression analyses performed.

Table S3: qPCR Primers

Gene	Purpose[a]	Site	Chromosomal location	Forward (5′ to 3′)	Reverse (5′ to 3′)
β-ACTIN	R	Exon 4	chr7:5534592-5534694	CCGGGACCTGACTGACTACCTCATG	CAGCTTCTCCTTAATGTCACGCACG
CIITA	C,D	-70.1 kb	chr16:10810219+10810311	TAAGAAATCTGTCTGTGGCA	TTCACAGAATTCCTCCGAAC
	C	-53.3 kb	chr16:10826971+10827065	ACCCTCCTGTTTGTATGGCT	CCTGAAGAAGGACTGGACTA
	C,D	-50.6 kb	chr16:10829702+10829775	CAGCTCATGTCCCACCCAGT	AACAAACATGTCAGGCCACAGT
	C	-43.4 kb	chr16:10836876+10836971	GCCATGAATCCTGCTCTAGACC	AGTTGCCTGAGCCGTGGTT
	C	-38.3 kb	chr16:10841978+10842059	GTGTCCTTGGGTTCTCTGCCT	GCCAGGAATTGCCTACACACTAGT
	C	-35.6 kb	chr16:10844650+10844739	CCAACAGGCAGGGTCATGCA	CAGCTTTGGTCTCAGGACACACCTA
	C	-32kb	chr16:10861288+10861417	GAAGTAGCCACTCCAGCAGA	TATGGATGCGGCTAAGGTGT
	C	-26.6kb	chr16:10853750+10853870	AATGAAGCTGCCATCCTTGCCA	TCTTCCTCAGTTGTTTCTTAGCCTAAGTCT
	C	-21.3 kb	chr16:10859024+10859094	ACTGGGCAGGACACATTGGT	TGGTCTCAAACTCTTGGGCG
	C,D	-16.4 kb	chr16:10863865+10863945	TTCTGCAACTAGGTAACACC	ATAGGTTGGATTACATGATC
	C	-13.8 kb	chr16:10866441+10866533	AATGGGCAGGAGAACAGTCG	CAGAGGATTTGCATAGAAGCCAG
	C	-12.3 kb	chr16:10867999+10868080	CTCTGAAAGGGAAGTCAATGGG	CCAAGTTTTCACTGCTCCTGC
	C	-11.8 kb	chr16:10868453+10868549	ACAGCCAGACATCCTGGTGG	GCTCATTGCAACCTCTGCCT
	C,D	-7.9 kb	chr16:10872386+10872455	AGTTGAACTGGCACATGGGC	CTCTTGGAATTGGGAAGGCA
	C	-6.3 kb	chr16:10873959+10874009	CCAGCTAAGCCCCCTTTACAAC	GTATGAGAACCTGGACCTGCTGAT
	C	-2.1kb	chr16:10878232+10878284	CATCCTGCAGAAGGTGGCA	CAATGGAACCGCACTGGTG
	C	-0.3 kb (pIV)	chr16:10879968+10880038	TCACGGTTGGACTGAGTTGG	CCTGAGTTGCAGGGAGCTTG
	D	-0.08 kb (pIV)	chr16:10880166+10880315	AGGCAGTTGGGATGCCACT	TCCGCTGGTCATCCTACCTC
	C	+1.8 kb	chr16:10882101+10882179	AGGCAATCAGGGAAGTGGCT	TTGTCAGTGTGACTCAAGGCAA
	C	+4.2 kb	chr16:10884481+10884569	GGACTGTGTTAAGTAGAGCCGGA	GTGGAGTGATGAGGATCTTGTGAC
	C	+6.3 kb	chr16:10886587+10886665	TGAGGAGCTTGCAGGTCAGA	TGAGCTTCGTGTCAGGAGAGG
	C	+10 kb	chr16:10948228+10948298	GGACGTAATCTCAGCGCCTG	TGTTAACGGCAACTCTGGGAG
	C	+19.1 kb	chr16:10899346+10899417	CACTCTGCCACTGTGACCCA	CAGGCCTTGAAAGATGAGGC
	C	+28.3 kb	chr16:10908568+10908638	AGGCCCAGGCATACGTGAT	CGTCAGGGCTCTGTCTTGGT
	C	+33.1 kb	chr16:10913529+10913631	GTGGTATGATCTTGGCTCAC	GGTGTAGTGGTGTACACCTG
	C	+40.0 kb	chr16:10920288+10920385	CACCTTCTGGTAGGCCTTGGCA	CCAAGCTCAGTCCGCTCATTACC
	C,R	+46.2 kb	chr16:10926464+10926533	ACGTCTGACAGGCAATGCTG	GGGTCCTAGCCAACTATTCCG
	C	+59.1 kb	chr16:10939330+10939420	CAGCCTGTCCTCTTCTGCTCACA	CGTGTTATACCCATGCCCTTGCAA
	C	+72.7 kb	chr16:10952931+10953055	AGATGCCTCAGCTCCCAGAGCA	ACTATGTATGTACCTCAGTA
	C	+82.6 kb	chr16:10962877+10962977	TTAGAGAAAGGCACTGGATGGTCTGT	GATACTTGTCTGTACACAGCCTAGCGG

a: R: RNA quantification. C: ChIP. D: DNase I accessibility.

Table S4: Antibodies

Target	Catalogue number	Source
H3ac	06-599	Upstate Biotechnology
H4ac	06-866	Upstate Biotechnology
BRG1	SC-10768	Santa Cruz
H3K4me2	07-030	Upstate Biotechnology
H3K4me3	07-473	Upstate Biotechnology
H3K79me3	ab2621	Abcam
Gal 4	06-262	Upstate Biotechnology
IRF1	SC-497	Santa Cruz
GFP	AA-11122	Invitrogen
P300	SC-584	Santa Cruz
Pol II	SC-9001	Santa Cruz
STAT1	06-501	Upstate Biotechnology

Table S5: 3C Primers

Looping between:	Chromosomal location	Primer (5′ to 3′)	Location	Amplicon Length (bp)
pIV and –50kb	chr16:10,879,952-10,879,971	GTGAAAGTGGCAAACCACCT	*CIITA* pIV	209
	chr16:10,829,457-10,829,476	CGGCTAGGTCACTTTCTCTA	*CIITA* -50 kb	
pIV and –8k	chr16:10,872,647–10,872,666	CAACGTGCATGGTGGAAAGA	*CIITA* –8kb	147
	chr16:10,879,919–10,879,938	GCCCCTGAGATGAGCTAACT	*CIITA* pIV	
pIV and *PITX2* Promoter	chr4:111,901,208–111,901,227	CTCGTCCATGAACTGCATGA	*PITX2* promoter	191
	chr16:10,879,917–10,879,936	CCCTGAGATGAGCTAACTGA	*CIITA* pIV	
pIV and +59kb	chr16:10,940,615–10,940,641	GACAACTAACAGCATCTGAGGTGGTGG	*CIITA* +59kb	317
	chr16:10,879,972–10,879,998	TCTGTTTCTCTCCAACTCAGTCCAACC	*CIITA* pIV	
pIV and –27kb	chr16:10,852,818–10,852,839	TATCTACAGGTCACTTTCCAGG	*CIITA* –27kb	143
	chr16:10,879,951–10,879,970	TGAAAGTGGCAAACCACCTC	*CIITA* pIV	
pIV and +28kb	chr16:10,908,507–10,908,526	CTGGTCCAGAGCCTGAGCAA	*CIITA* +28kb	120
	chr16:10,879,901–10,879,920	CTGAGCTATTCACTCCTCTG	*CIITA* pIV	
pIV and +47kb	chr16:10,927,641–10,927,660	CCATCCAGGTTCAGCTTGTA	*CIITA* +47kb	113
	chr16:10,879,871–10,879,890	TAGGGAGGAAGAGAAAATCC	*CIITA* pIV	
pIV and –16kb	chr16:10,864,261–10,864,283	AATGTAGAACTCAGGATGAACAT	*CIITA* 16kb	159
	chr16:10,879,919–10,879,938	GCCCCTGAGATGAGCTAACT	*CIITA* pIV	
+59kb and –50kb	chr16:10,940,710–10,940,736	AATGGGATTGTGTCATCTCCTGCCTAG	*CIITA* +59kb	172
	chr16:10,829,450–10,829,476	CGGCTAGGTCACTTTCTCTAGTAGGGA	*CIITA* –50kb	
+59kb and –73kb	chr16:10,940,732–10,940,758	CCTAGAACCTTCCAATGGCTTTCCACT	*CIITA* +59kb	143
	chr16:10,806,865–10,806,891	ATCCATGAACATGATTTGTGGCTGTCT	*CIITA* –70kb	
+59kb and 47kb	chr16:10,940,615–10,940,641	GACAACTAACAGCATCTGAGGTGGTGG	*CIITA* +59kb	252
	chr16:10,927,641–10,927,660	CCATCCAGGTTCAGCTTGTA	*CIITA* +47kb	
+59kb and –27kb	chr16:10,940,615–10,940,641	GACAACTAACAGCATCTGAGGTGGTGG	*CIITA* +59kb	202
	chr16:10,852,818–10,852,839	TATCTACAGGTCACTTTCCAGG	*CIITA* –27kb	
+59kb and 16kb	chr16:10,940,710–10,940,736	AATGGGATTGTGTCATCTCCTGCCTAG	*CIITA* –16kb	183
		GTCTGCGTTCTTGAGGGATATTTGCAC	*CIITA* +59kb	
+59kb and 8kb	chr16:10,864,232–10,864,258	ATGGGATTGTGTCATCTCCTGCCTAGA	*CIITA* –8kb	138
	chr16:10,940,711–10,940,737	GTGCATGGTGGAAAGATGACTGTAAGT	*CIITA* +59kb	
	chr16:10,872,651–10,872,677			
–50kb and –16kb	chr16:10,864,261–10,864,283	AATGTAGAACTCAGGATGAACAT	*CIITA* –16kb	120
	chr16:10,829,408–10,829,427	CTAAGGGAGCGACCAGTGTC	*CIITA* –50kb	
–50kb and –8kb	chr16:10,829,411–10,829,430	CTGCTAAGGGAGCGACCAGT	*CIITA* –50kb	121
	chr16:10,872,637–10,872,656	ACCACAAGCCCAACGTGCAT	*CIITA* –7.9kb	
–50kb and +47kb	chr16:10,829,411–10,829,430	CTGCTAAGGGAGCGACCAGT	*CIITA* –50kb	125
	chr16:10,927,641–10,927,660	CCATCCAGGTTCAGCTTGTA	*CIITA* +47kb	
–50kb and –27kb	chr16:10,852,818–10,852,839	TATCTACAGGTCACTTTCCAGG	*CIITA* –27kb	121
	chr16:10,829,457–10,829,476	CGGCTAGGTCACTTTCTCTA	*CIITA* –50kb	
–16kb and –8kb	chr16:10,864,261–10,864,283	AATGTAGAACTCAGGATGAACAT	*CIITA* –16kb	140
	chr16:10,872,647–10,872,666	CAACGTGCATGGTGGAAAGA	*CIITA* –7.9kb	
–16kb and +47kb	chr16:10,864,261–10,864,283	AATGTAGAACTCAGGATGAACAT	*CIITA* –16kb	154
	chr16:10,927,641–10,927,660	CCATCCAGGTTCAGCTTGTA	*CIITA* +47kb	
–8kb and +47kb	chr16:10,872,647–10,872,666	CAACGTGCATGGTGGAAAGA	*CIITA* –7.9kb	142
	chr16:10,927,641–10,927,660	CCATCCAGGTTCAGCTTGTA	*CIITA* +47kb	
–8kb and –27kb	chr16:10,872,647–10,872,666	CAACGTGCATGGTGGAAAGA	*CIITA* –7.9kb	92
	chr16:10,852,818–10,852,839	TATCTACAGGTCACTTTCCAGG	*CIITA* –27kb	

Table S6: Recombineering oligonucleotides

Forward[a]	Reverse[a]	Location at *CIITA* locus	Replaced Length (bp)
CACAATGGCCAGACTCCAAGATTTTCA GAAACTTCCAAGCCTCTTCCTGG CCTGTTGACAATTAATCATCGGCA	TGTTGTTGCTTTGGATACACAGGAAGGA GAGAGATGGGCAGTGACTCCCC TCAGCACTGTCCTGCTCCTT	–50kb chr16:10829543+10830632	889
CTCATAATGCCCATGTGTAAGAATTTTT CTGGCATATATACTGAAGAGTGGAAAT CCTGA CCTGTTGACAATTAATCATCGGCA	TAACACAGTACATATAGAACACCTGAAT GATCACCGACTTCTTGTTTGAAACCATGG CGG TCAGCACTGTCCTGCTCCTT	–16kb chr16:10863261+10864390	929
CCAGCCTGATGATTCAGAAGTCCCCTTC AGATATTGCAGTGCCTTAGGTGCAATT GTGCA CCTGTTGACAATTAATCATCGGCA	GTAGATTACCACCATAAGACAGGGCGAG AGGCTGGGCACAGTGGCTCACGCCTATA ATCC TCAGCACTGTCCTGCTCCTT	–8kb chr16:10871640+10873809	1969
CATGAGCAAAGTGCTAACTGGTGCAAC TGGTGAGTTTGGGCGGGCATTGTTTGTG CTCTT CCTGTTGACAATTAATCATCGGCA	CAAGTGCCGAGGAAGCTCAGAACCCCAG GGTATGAGAGGGGTAGCTAGCAGCAGGG AAGC TCAGCACTGTCCTGCTCCTT	+59kb chr16:10937861+10940030	1969
AGCACATGCCCAATGTCCCAGGCAAGC TGTGGCTCTGCACCTGTGGGCTCCATCC ACCGGGGCCAGGGTG CCTGTTGACAATTAATCATCGGCA	ACGTCAGCACCATCACCTCAGATTATTCC ACCACATCGTCTGCTACATACTTGACTAG CCTGGACTCCAG TCAGCACTGTCCTGCTCCTT	–39kb chr16:10840423+10842882	2319
AGTCTCAAAGTTGGTAAATTTTACGCC AAAGCTCACGATACTTGCCTTCTTTCCC TTCTCAATTTATTTC CCTGTTGACAATTAATCATCGGCA	GATTACAGGTGTGAGCCACCACACCCGG CCCAGAGACCCATTTTCTTTCACGCATCC ACAGCTTTCACTG TCAGCACTGTCCTGCTCCTT	+13kb (Intron 1) chr16:10892330+10893429	959
GCCCTGAACAAAAGGATTAGCGGGACG TGGTGAAAGAAACTCTGAGCAAGTCAG TTATTCATTCCTAGCC CCTGTTGACAATTAATCATCGGCA	GTGATCATGCTGGGAAGAAATTAACAAG GCTCAGGAGGGTATAGGACCCAGCTACT TGGAAGGCTGAGGT TCAGCACTGTCCTGCTCCTT	+40kb (Intron 16) chr16:10919998+10921048	910

a: Primers were selected to both avoid repetitive DNA and to replace a length of sequence as close to the *galK* gene (1.2 kb) as possible. *galK* gene primers are underlined.

Table S7: BAC quantification primers

Region	Primer location	Forward (5′ to 3′)	Reverse (5′ to 3′)	Amplicon Length (bp)
BAC	*Luciferase*	TTGTGCCAGAGTCCTTCGATA GGGA	GTTCTATGAGGCAGAGCGAC ACCTT	100
	galK	TCGCGCTTAACGGTCAGGAA	GGCAATCGATCAGCAAGGCA	114
	Kanamycin	CTTGCTCCTGCCGAGAAAGTA TCCA	ACCGGCTTCCATCCGAGTACG TGCT	135
	Sop	GGTGATAGTGTTGAGAAGAC	TATGACACCAGATACTCTTC	153
Genomic DNA	Chr 1:*IFI16* promoter	AAGCCCAGGCTTGTCAGTTAT TAAT	AGGAGGAGATCTTGGTAGGA GCATCT	146
	Chr 5: *IRF1* promoter	GCTAAGTGTTTGGATTGCTCG GTGG	TTGCCTCGACTAAGGAGTGGC GAGC	68
	Chr 19: *JunB* 3′ UTR	CCAGCTCAAACAGAAGGTCA TG	GACGTTCAGAAGGCGTGTCC	84

SUPPLEMENTAL EXPERIMENTAL PROCEDURES

Plasmid Construction

pREP4–Luc was from K Zhao [1]. A 379 bp human *CIITA* pIV fragment was amplified using the primers o–hCA–12 (5′ –CCCGGTACCGGAGAGAAACAGAGACCCAC–3′, Knp I site underlined) and hCA–13 (5′–GGCAAGCTTCCTCTCCCTCCCGCCAGCTC–3′,Hind III site underlined), digested with Kpn I and Hind III and ligated to Kpn I/Hind III–digested pREP4–Luc, to generate pREP4–pIV–Luc. pREP4–8kb was derived from a non–replicating version called pCIITAproIV(8800) (a gift from J.F. Piskurich) [2]. A 7.8 kb fragment from pCIITApropIV(8800) digested with BamHI/PmlI was inserted into pREP4–pIV–Luc digested by Bgl II/Pml I, generating pREP4–8kb–Luc. To insert the –50kb remote site in pREP4–pIV–Luc, a 1053 bp fragment was amplified by the primers hCA–50kben–5BglII (5′ –CGC AGATCT ACTTCCAAGCCTCTTCCTGG–3′, restriction enzyme sites underlined, same for the following) and hCA–50kben–6BglII–NheI (5′–CGC AGATCT GCTAGC GCTTTGGATACACAGGAAGG–3′), which was then digested with Bgl II and ligated to Bgl II–digested pREP4–pIV–Luc to generate pREP4–50kb–pIV–Luc. To add the –16kb fragment upstream of pIV in pREP4–pIV–Luc, a 1011 bp fragment was amplified with the primers hCA–16kben–5NheI–KpnI (5′–GC GGTACC ATA GCTAGC CATTACCAAATTACTACCCT–3′) and hCA–16kben–6NotI–KpnI (5′–TAT GGTACC TAT GCGGCCGC ACTTCTTGTTTGAAACCATG–3′), which was digested with Kpn I and ligated to Kpn I–digested pREP4–Luc–pIV to generate pREP4– 16kb–pIV–Luc. To insert the –16kb element between –50kb and pIV a 1011 bp fragment was amplified using hCA–16kben–5NheI (5′–CGC GCTAGC CATTACCAAATTACTACCCT–3′) and hCA–16kben–6NotI–KpnI (5′–TAT GGTACC TAT GCGGCCGC ACTTCTTGTTTGAAACCATG–3′), digested with Nhe I/Kpn I and ligated to Nhe I/KpnI–digested pREP4– pIV–50kb–Luc to generate pREP4–50–16–pIV–Luc. The latter has Nhe I and Not I sites at the 5′ and 3′–end of –16 kb fragment, respectively. To add the –8kb fragment between –16kb and pIV in pREP4– 50kb–16–pIV–Luc construct, a 1636 bp fragment amplified by hCA–7.8kben–5NotI (5′–ATA GCGGCCGC TGGGAAGTTAAAGCAAACAT–3′) and hCA–7.9kben–6–AgeI–KpnI (5′–CGC GGTACC TAT ACCGGT AAAGACAGGGTGAGAATAAT–3′) was digested with Not I/Kpn I and ligated to Not I/KpnI–digested pREP4– 50–16kb–pIV–Luc construct to generate pREP4– 50–16–8kb–pIV–Luc. A pREP4–Luc–8kb–pIV construct was generated by digesting pREP4–Luc–50kb–16–8kb–pIV with Bgl II/Not I, followed by Klenow treatment and ligation. All the clones were sequence verified.

Chromosome conformation capture (3C).

The 3C assay was conducted as described [3] with minor modifications. Briefly: cells were cross–linked with 2 % formaldehyde for 10 minutes at room temperature in a buffer containing 10 mM

Tris–Cl pH 7.9, 10 mM $MgCl_2$, 50 mM NaCl and 1 mM dithiothreitol. The reaction was quenched by addition of glycine to 0.125 M. SDS was added to a final concentration of 0.1 % and incubated at 37°C for 10 minutes in order to remove any non–cross–linked proteins from the DNA. To sequester SDS and allow subsequent restriction digestion, Triton X–100 was added to a final concentration of 1%. The DNA was digested with the restriction enzyme Nco I for one hour at 37°C in a final volume of 50 μl. The restriction enzyme was inactivated by adjusting to 1.6 % SDS and incubation at 65°C for 20 minutes. 20–40 ul was diluted into 800 μl of ligation buffer, Triton–X added to a final concentration of 1% and incubated for 1 hr at 37°C. T4 ligase added and ligation performed over night at 16°C. The cross–links were reversed overnight at 65°C in the presence of 5 μg/ml Proteinase K and the DNA was purified by phenol–chloroform extraction and ethanol precipitation. PCR was conducted using primers flanking the desired fragments. PCR products were confirmed on 1.5% agarose gels containing 0.75 μg/ml ethidium bromide.

To quantify 3C ligation, standards were generated as described [4]. In brief, 30 μg of CTD–2577P18 BAC DNA were digested with 300 units of NcoI overnight at 37°C. DNA was phenol/chloroform extracted and ethanol precipitated. DNA fragments were ligated with T4 DNA ligase at high concentration (300 ng/μl) thus generating equimolar amounts of all possible ligation products. DNA was purified by phenol–chloroform extraction and ethanol precipitation. Calibration samples were prepared in the range of 0.00001 to 0.5 ng/μl covering the dynamic ranges of amplified experimental templates. 200 ng of the cross–linked DNA/PCR were used in qPCR reactions, which was within the linear range and produced minimal within–sample variability. The relative cross–linking frequencies were calculated by interpolating the PCR signal of the cross–linked DNA of a specific PCR product onto the respective standard curve, thus correcting for any differences in PCR amplification efficiencies. The data was presented as fold above the cross–linking frequency with an irrelevant control site and was reproduced in 3–6 independent experiments. Looping frequency between the different NcoI fragments was statistically evaluated relative to the background signal of contact with the negative control elements (–27, +28kb) using one way ANOVA followed by Fisher test.

To determine if loops detected reflected linear proximity and thus non–specific collisions, we first graphed the interaction frequency between each NcoI fragment and other fragments within a 30 kb distance up or downstream. The analysis was carried out twice: in one case, distance between fragments was taken as the length between the closest ends of each fragment, while in the second case distance between fragments was taken as the length between the centre of each fragment (**Fig S5** shows

the former analysis, but the latter process generates similar graphs). These analyses were carried out for the data in untreated or IFN-γ treated HeLa cells (**Fig S5b**), or for SW13 cells +/– BRG1 and +/– IFN-γ (**Fig S5c**). From the graphs, it is visually apparent that proximity does not define positive interactions. For example, in HeLa or SW13 cells the interaction between D (–8) and E (pIV) is very strong, yet it is low between C (–16) and D (–8) which are closer together, and it is also low between G (+40) and H (+59), which are a similar distance apart as D and E (**Fig S5**). Moreover, in HeLa, a robust interaction was detected between fragments C (–16) and E (pIV) that are ~15 kb apart, but low level contacts were made between several other fragments that are similar distances apart (**Fig S5b**). The longer–range interaction between fragments E and G that are ~ 29 kb apart is also much stronger than that between many closer fragments (**Fig S5**). As a second test, we calculated the correlation coefficients for distance versus interaction frequency for all 21 interactions that were assessed. This analysis was also performed for all data sets, including HeLa +/– IFN-γ, as well as SW13 +/– BRG1 and +/– IFN-γ. In every case, R^2 was extremely low (**Supplementary Table 2**), again indicating that looping is not randomly linked to proximity at *CIITA*. We also observed no correlation between distance and contact at the SOCS1 locus (MAEH and RB, unpublished data). Furthermore, this gene is not induced in SW13 cells and in line with this perpetually silent state we detect no looping, even between the closest fragments (MAEH and RB, unpublished data). Altogether, these analyses present a strong case that the interactions detected at *CIITA* are functionally relevant and not a non–specific consequence of linear proximity.

Recombineering

Preparation of BAC DNA. Bacteria carrying the human BAC, CTD–2577P18, was streaked for single colonies and characterized by PCR and restriction analysis (EcoRV digestion) before proceeding to the recombineering experiments. BAC minipreps were used for small scale preparations (1–1.5 µg). Briefly, 5 ml overnight LB culture was pelleted for 5 min at 5000 rpm, and the supernatant removed. The pellet was dissolved in 250 µl buffer P1 (miniprep kit, Qiagen) and transferred to an eppendorf tube. An aliquot of 250 µl P2 buffer was added followed by mixing by inversion and incubation for <5 min at room temperature. An aliquot of 250 µl N3 buffer was added followed by mixing and incubation on ice for 5 min. The supernatant was cleared by two rounds of centrifugation at 13 200 rpm for 5 min in a tabletop centrifuge. Each time the supernatant was transferred to a new tube. DNA was precipitated by adding 750 µl isopropanol, mixing and incubating on ice for 10 min, and centrifugation for 10 min at 13200 rpm. The pellet was washed once in 70% ethanol and the dry pellet was dissolved in 50 µl TE.

An aliquot of 40 µl (~1µg) was used for restriction analysis, and 1 µl was used as template for PCR analysis or transformation of electrocompetent bacteria. Large–scale preparations of BAC DNA (25–100 µg) were done using the NucleoBond BAC Maxi kit (Clontech, Cat# 635941) following the manufacturer's instruction.

Introduction of BAC DNA into SW105 cells. SW105 *E. coli.* cells were transformed with CTD2577P18 BAC DNA by electroporation. These bacteria contain λ Red genes that facilitate recombination. λ Red expression is induced by a temperature shift from 32°C to 42°C. To prepare bacteria for electroporation, 500 µl of an overnight culture was diluted in 25 ml Luria–Bertani (LB) medium with chloramphenicol selection (12.5µg/ml) in a 50 ml baffled conical flask and grown at 32°C with shaking to an OD_{600} of 0.6. Then, 10 ml was transferred to another baffled 50 ml conical flask and heat–shocked at 42°C for exactly 15 minutes in a shaking waterbath. The remaining culture was left at 32°C as the uninduced control. Next, the bacterial samples were briefly cooled in ice–water slurry and then transferred to two 15 ml Falcon tubes and pelleted at 5000 rpm at 0°C for 5 minutes. The supernatant was poured off and the pellet was resuspended in 1 ml ice–cold ddH_2O by gently swirling the tubes in an ice waterbath slurry. Subsequently, the sample was washed twice with 9 ml ice–cold ddH_2O. After the second washing and centrifugation step, the supernatant was removed, and the pellet (~50 µl each) was kept on ice until electroporated with DNA. An aliquot of 25 µl, in combination with DNA fragments, was used for each electroporation in a 0.1 cm cuvette (BioRad) at 25 µF, 1.75 kV and 200Ω. After electroporation, the bacteria were recovered in 1 ml LB (15 ml Falcon tube) for 1 h at 32°C with shaking.

Recombineering to generate BAC–*CIITA*. A Luc reporter BAC was constructed using recombineering [5, 6]. First, classic cloning approaches were used to replace the GFP gene in pIGCN21 plasmid (from N. Copeland) with the firefly Luc gene from pGL3 (Invitrogen), thus creating pIGCN21–Luc. The Luc fragment was amplified by the forward primer CCG CCACAACC ATGG AAGACGCCAAAAACATAA (Bst XI site underlined), and reverse primer CCG CCCGGG TTACACGGCGATCTTTCCGC (Xma I site underlined), and was inserted into pIGCN21 digested with Bst XI/Xma I. Next, this plasmid was modified to place homology arms corresponding to adjacent sequences in the last exon (exon 20) of *CIITA* either side of the IRES–Luc–FRT–kan^r–FRT cassette. 333 bp and 306 bp *CIITA* sequences were amplified by two pairs of primers. The first 333 bp 5′ fragment was amplified by the primers: forward GCG GTCGAC AAGAGCTTCCTTTGGGGACT (Sal I site underlined), and reverse CCG CTGCAG AAGTACCCAGTTCAAGGTCCAGC (Pst I site underlined). The second 306 bp 3′ homology arm was amplified by the primers: forward CAA

GGCCGAGGCGGCC CGCTGGACCTTGAACTGGGTAC (Sfi I site underlined), and reverse CGA GAGCTCT GGGCAGGCAGAATGGGGCT (Sac I site underlined). These two fragments were ligated into pIGCN21–Luc digested by Sal I/Pst I, and Sfi I/Sac I, respectively. The 5′ *CIITA* arm–IRES–Luc–FRT–kan^r–FRT–3′ homology arm cassette was excised using Sal I/Sac I. This fragment was inserted into the BAC–*CIITA* by recombineering in SW105 cells. Recombined colonies were selected in Kanamycin and junctions verified by PCR and restriction enzyme digests. The *Kan/Neo* gene is flanked by FLP–recognition target (*FRT*) sites, thus to continue using the kan^r selection marker in the next construction step, the *Kan/Neo* gene was removed by adding arabinose which induces Flpe expression in SW105 bacteria. Next, a replication origin that functions in mammalian cells (SV40ori–S/MAR) was introduced into the BAC backbone. The SV40ori–S/MAR cassette was present in the plasmid pEPI–GFP, a gift from Dr. H. Lipps and a derivative of pEPI–1 plasmid, which contains the ~2kb S/MAR fragment from the 5′ regions of the human IFN-β gene [7]. First, sequences flanking but not including the loxP site in the BAC backbone were amplified to generate homology arms (this strategy was designed so that the final recombineered BAC vector would lack the loxP site). The 5′– BAC homology arm was amplified by the forward primer: CGC GCTAGC GCGGCCGC CACGGTCCCACTTGTATTGT (Nhe I and NotI underlined), and reverse primer: CGC AGATCT GACAATACAAATCAGCGACA(Bgl II underlined). The 3′– BAC homology arm was amplified by the forward primer: CCG CCACCGAGACC TTCGCGTCAGCGGGTGTTGG (Bsa I underlined), and reverse primer: CGC AGGGCCT GCGGCCGC CCGTCGTTTTACAACGTCGT (Eco O109I and NotI I underlined). These two fragments were ligated into into pEPI–EGFP using Nhe I/ Bgl II and Bsa I/Eco O109I digestion, respectively. The 5′ homology arm–SV40ori–S/MAR–*Kan/Neo*–3′ homology arm cassette was excised using Not I and introduced into the BAC vector by recombineering. Colonies were selected in Kanamycin and junctions verified by PCR and restriction enzyme digestion.

Construction of BAC–*CIITA* deletion mutations**.** *galK* selection was performed as described by Warming et. al. based on the principle that SW105 bacterial cells die in galactose minimal media but are rescued by *galK* [6]. First, PCR was conducted to obtain the *galK* gene flanked by 50–70 bp homology arms located at either side of the –50, –16, –8 +40, and +59 kb remote elements and –39 and +13 kb control loci at *CIITA*. The resulting DNA fragments were used in recombineering as above. The electroporated bacteria were recovered in 1 ml LB and incubated for 1 h in a 32°C with shaking. After the recovery period, the bacteria were washed twice in 1x M9 salts as follows: 1 ml culture was pelleted in an eppendorf tube at 13,200 rpm. for 15 seconds and the supernatant was removed. The pellet was resuspended in 1 ml of 1x M9 salts, and pelleted again. This washing step was repeated once more. After the second wash, the supernatant was removed and the pellet was

resuspended in 1 ml of 1x M9 salts before plating serial dilutions (100 µl, 100 µl each of 1:10, and 1:100 dilutions) on glactose minimal medium M63–agar plate (15 g/l agar; 0.2% D–galactose, Sigma; 1 mg/l D–biotin, Sigma; 45 mg/l L–leucine, Sigma; and 12.5 µg/ml chloramphenicol , Sigma). The uninduced samples routinely had a higher degree of lysis/bacterial death after electroporation, so the uninduced samples were diluted in 0.5 ml 1x M9 salts in the final step to make up for the difference. After 3 to 7 day incubation, several colonies were picked and inoculated into *gal* indicator plates (MacConkey agar, Bioshop; 1% D–galactose; and 12.5 µg/ml chloramphenicol). The bright red colonies were chosen for further verification by PCR and restriction enzyme digestion.

Generation of BAC SW13 clones, quantification of BAC DNA and normalization of Luc data

SW13 cells were transfected with 5 µg of BAC DNA for 24 hrs using lipofectin (Invitrogen) according to the manufacturer's instructions. Media was replaced and cells were incubated for an additional two days. Cells were then trypsinized, replated and stable clones selected in 500 µg/ml of G418. Total genomic DNA and BAC DNA was prepared from 4 x10^5 cells. Cells were lysed in 250 µl of genomic DNA extract cell lysis solution (0.6% SDS, 100 mM NaCl, 50 mM Tris.Cl (pH 8), 20 mM EDTA, and 50 µg/ml RNase A) and the plate rocked gently at room temperature for 20 minutes. Lysates were transferred to a microfuge tube, and incubated at 37°C for1 hr, then proteinase K was added to a final concentration of 100 µg/ml and incubated at 55°C overnight. The lysate was then extracted twice with phenol:chloroform (1:1), and twice with chloroform. DNA was precipitated with 30 µl of 5 M NaCl and 1.3 ml of absolute ethanol, chilled on ice for 5 minutes and pelleted at 13,000 rpm for 30 minutes at 4°C. Finally, the DNA pellet was washed with 70% ethanol, air–dried briefly and resuspended in 20 µl of TE.

BAC and genomic DNA copy number was quantified by qPCR using three primer sets specific for BAC DNA (*Kan, Luc and Sop*), and three for genomic DNA (*IFI16* promoter, *IRF1* promoter and *JunB* last exon on chromosomes 1, 5 and 19 respectively). BAC copy numbers were averaged and normalized to the average of the three genomic segments. Raw values from Luc assays were normalized to protein content, then to the normalized BAC copy number. The overall formula used was: (Raw Luc activity/Protein level)/(Average of three BAC amplicons/Average of three genomic amplicons).

Supplemental References

1. Liu, R. *et al.* Regulation of CSF1 promoter by the SWI/SNF–like BAF complex. *Cell* **106**, 309–318. (2001).
2. Piskurich, J.F., Wang, Y., Linhoff, M.W., White, L.C. & Ting, J.P. Identification of distinct regions of 5' flanking DNA that mediate constitutive, IFN–gamma, STAT1, and TGF–beta–regulated expression of the class II transactivator gene. *J Immunol* **160**, 233–240. (1998).
3. Dekker, J., Rippe, K., Dekker, M. & Kleckner, N. Capturing chromosome conformation. *Science* **295**, 1306–1311 (2002).
4. Spilianakis, C.G., Lalioti, M.D., Town, T., Lee, G.R. & Flavell, R.A. Interchromosomal associations between alternatively expressed loci. *Nature* **435**, 637–645 (2005).
5. Copeland, N.G., Jenkins, N.A. & Court, D.L. Recombineering: a powerful new tool for mouse functional genomics. *Nat Rev Genet* **2**, 769–779 (2001).
6. Warming, S., Costantino, N., Court, D.L., Jenkins, N.A. & Copeland, N.G. Simple and highly efficient BAC recombineering using galK selection. *Nucleic Acids Res* **33**, e36 (2005).
7. Piechaczek, C., Fetzer, C., Baiker, A., Bode, J. & Lipps, H.J. A vector based on the SV40 origin of replication and chromosomal S/MARs replicates episomally in CHO cells. *Nucleic Acids Res* **27**, 426–428. (1999).